

Summer 2015

A non-invasive fluorescence-based oxygen sensor and platform for studying cell responses to metabolic agents in real-time

Koutilya Reddy Buchapudi
Louisiana Tech University

Follow this and additional works at: <https://digitalcommons.latech.edu/dissertations>



Part of the [Bioimaging and Biomedical Optics Commons](#)

Recommended Citation

Buchapudi, Koutilya Reddy, "" (2015). *Dissertation*. 191.
<https://digitalcommons.latech.edu/dissertations/191>

This Dissertation is brought to you for free and open access by the Graduate School at Louisiana Tech Digital Commons. It has been accepted for inclusion in Doctoral Dissertations by an authorized administrator of Louisiana Tech Digital Commons. For more information, please contact digitalcommons@latech.edu.

**A NON-INVASIVE FLUORESCENCE-BASED OXYGEN SENSOR
AND PLATFORM FOR STUDYING CELL RESPONSES
TO METABOLIC AGENTS IN REAL-TIME**

by

Koutilya Reddy Buchapudi, B.Tech., M.S.

**A Dissertation Presented in Partial Fulfillment
of the Requirements for the Degree
Doctor of Philosophy**

**COLLEGE OF ENGINEERING AND SCIENCE
LOUISIANA TECH UNIVERSITY**

August 2015

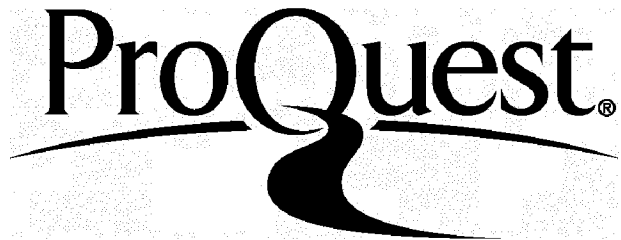
ProQuest Number: 3664523

All rights reserved

INFORMATION TO ALL USERS

The quality of this reproduction is dependent upon the quality of the copy submitted.

In the unlikely event that the author did not send a complete manuscript and there are missing pages, these will be noted. Also, if material had to be removed, a note will indicate the deletion.



ProQuest 3664523

Published by ProQuest LLC(2015). Copyright of the Dissertation is held by the Author.

All rights reserved.

This work is protected against unauthorized copying under Title 17, United States Code.
Microform Edition © ProQuest LLC.

ProQuest LLC
789 East Eisenhower Parkway
P.O. Box 1346
Ann Arbor, MI 48106-1346

LOUISIANA TECH UNIVERSITY
THE GRADUATE SCHOOL

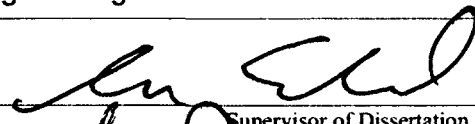
June 8th, 2015

Date

We hereby recommend that the dissertation prepared under our supervision
by Koutilya Reddy Buchapudi

entitled A Non-Invasive Fluorescence-Based Oxygen Sensor and Platform for Studying
Cell Responses to Metabolic Agents in Real-Time

be accepted in partial fulfillment of the requirements for the Degree of
Doctor of Philosophy in Biomedical Engineering

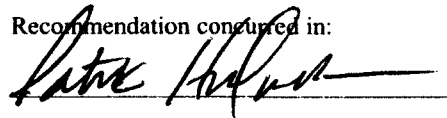


Supervisor of Dissertation Research

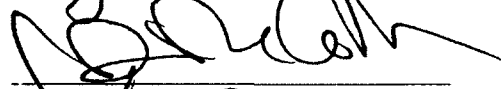

Head of Department
Biomedical Engineering

Department

Recommendation conferred in:









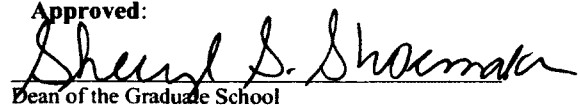
Advisory Committee

Approved:



Director of Graduate Studies

Approved:



Dean of the Graduate School



Dean of the College

ABSTRACT

A fluorescence-based sensor in a transverse flow/stop measurement platform has been developed to determine real-time changes in oxygen consumption rates for cell metabolic studies. The oxygen sensitive fluorophore platinum octaethylporphyrin was embedded in a cellulose acetate matrix and affixed to a fiber optic bundle, which provided for transmission of the excitation and emission wavelengths of the film. The fiber optic bundle was sealed in a sensor head that can be used in standard 24-well plates common to research labs. The utility of the sensor and sensing platform were determined by measuring the changes in oxygen consumption rates of *Candida albicans* during 90/30 s flow/stop cycles. Exposure of these cells to metabolic antagonists and an enhancer showed the expected decrease and increase in oxygen consumption rates in real time. The applicability of the platform to biological studies is illustrated by determination of synergistic activities between antifungal drugs and fluoride exposure in *Candida albicans*. The robustness of the fluorophore film is demonstrated by perfusion with different media and analyte conditions in the absence of cells. For stop cycle time intervals less than 1 minute the sensor exhibited a rapid and fairly linear change in fluorescence intensity to changing oxygen concentrations in the measurement chamber. Flow cycle fluorescence intensities were used as a baseline correction for treating the stop cycle fluorescence peaks.

APPROVAL FOR SCHOLARLY DISSEMINATION

The author grants to the Prescott Memorial Library of Louisiana Tech University the right to reproduce, by appropriate methods, upon request, any or all portions of this Dissertation. It is understood that "proper request" consists of the agreement, on the part of the requesting party, that said reproduction is for his personal use and that subsequent reproduction will not occur without written approval of the author of this Dissertation. Further, any portions of the Dissertation used in books, papers, and other works must be appropriately referenced to this Dissertation.

Finally, the author of this Dissertation reserves the right to publish freely, in the literature, at any time, any or all portions of this Dissertation.

Author Koutilya R Buchapudi

Date 07/17/15

DEDICATION

I dedicate this dissertation to my wife, Deepika Bandhanadham, and thank her for all the support.

TABLE OF CONTENTS

ABSTRACT	iii
DEDICATION	v
LIST OF FIGURES.....	ix
ACKNOWLEDGMENTS.....	xiv
1.0 INTRODCUTION	1
1.1 Motivation.....	1
1.2 Cell Metabolic Measurements	2
1.3 Cytosensor® Microphysiometer	4
1.4 Fluorescence Spectroscopy	9
1.5 Fluorescence Instrumentation	12
1.6 Fluorophores for Detecting Oxygen	15
2.0 PLATFORM DESIGN.....	20
2.1 Introduction.....	20
2.2 Platform 1.....	20
2.2.1 Prototype 1 Response to 0% Oxygen Water	22
2.3 Platform 2.....	27
2.3.1 Prototype 2 Response to 0% Oxygen Water	28
2.4 Protocol for Plating <i>C. albicans</i> in a 24-Well Plate	31
3.0 SENSOR RESPONSE TO METABOLIC ANATAGONOST AND ENHANCER	35

3.1 Introduction.....	35
3.1.1 Fluorescence-Based Sensors	35
3.1.2 Discontinuous Transverse Flow Platform	37
3.1.3 Platform Test Sensor: Oxygen	38
3.2 Materials and Methods.....	39
3.2.1 Materials.....	39
3.2.2 PtOEP Film Preparation	39
3.2.3 Sensor Head Construction	40
3.2.4 Cell Culture and Plating	41
3.2.5 Experimental Set-up and Conditions.....	42
3.3 Results and Discussion	42
3.3.1 PtOEP Film Response to 0% Oxygen and Ambient Oxygen Water.....	42
3.3.2 PtOEP Film Response With Cells.....	43
3.3.3 PtOEP Film Response During Different Flow/Stop Cycles With Cells	44
3.3.4 PtOEP Film Response With No Cells	46
3.3.5 Response of Sensor to Changing Oxygen Consumption Rates.....	48
3.3.6 Conversion of Raw Data To Normalized Peak Height	50
3.3.7 Response of Sensor to Different Concentrations of NaF.....	50
3.3.8 Response of Sensor to DNP	52
3.3.9 C. albicans Response to Glucose Stimulation.....	53
3.4 Conclusions.....	54

4.0 C. ALBICANS RESPONSE TO ANTIFUNGALS	56
4.1 Introduction.....	56
4.2 Materials and Methods.....	59
4.2.1 Materials	59
4.2.2 Cell Culture	59
4.3 Results and Discussion	59
4.3.1 Correlation Between PtOEP Polymer Film, Oxygen, and Cells.....	59
4.3.2 C. albicans Response to NaF	60
4.3.3 C. albicans Response to Amphotericin B	61
4.3.4 C. albicans Response to Miconazole	64
4.3.5 C. albicans Response to Fluconazole	65
4.4 Conclusions.....	67
5.0 FUTURE WORK.....	69
6.0 REFERENCES	72

LIST OF FIGURES

Figure 1.1.	Simplified extra- and intracellular metabolic cell model highlighting glycolysis [4].	2
Figure 1.2.	Cytosensor [®] Microphysiometer pH sensor cell setup [17].	4
Figure 1.3.	Acidification rate measurements using the Cytosensor [®] Microphysiometer [2].	5
Figure 1.4.	Top left: modified Cytosensor [®] Microphysiometer sensor head with four (A, B, C, D) platinum electrodes. Top right: the electrochemical measurement setup. Bottom: changes in oxygen and glucose consumption and lactate production rates of CHO cells in respiration [2].	7
Figure 1.5.	Jablonski diagram [32]	10
Figure 1.6.	Excitation spectrum of a fluorophore and the resulting fluorescence emission spectra at different excitation wavelengths [33].	12
Figure 1.7.	General schematic of a spectrofluorometer [34].	13
Figure 1.8.	Portable USB4000 FL Spectrometer and its Components. 1) SMA 905 Connector 2) Entrance slit 3) Filter 4) Collimating Filter 5) Grating 6) Focusing Mirror 7) Detector Collection Lens 8) Detector 9) Filter 10) Detector. Dimensions of an Ocean Optics 4000 FL Spectrometer are 89.1 mm x 63.3 mm x 34.4 mm [35].	14
Figure 1.9.	Clark electrode: (A) Pt-electrode, (B) Ag/AgCl-reference, (C) KCl electrolyte, (D) Teflon membrane, (E) rubber ring, (F) voltage supply, (G) galvanometer [37].	15
Figure 1.10.	Structure of platinum-octaethylporphyrin (PtOEP) [42].	17

Figure 1.11. Response times and relative intensity changes for (a) PtOEP and (b) PdOEP immobilized in poly-Sty1-co-PFS0.21 film on switching between 100% argon (1) and 100% oxygen (2) for 300 s. The excitation wavelengths for PtOEP and PdOEP were 535 and 546 nm, respectively, and the emission wavelengths were 645.4 and 663.8 nm, respectively [43].	18
Figure 2.1. Experimental set up for Prototype 1. Components are not to scale.	21
Figure 2.2. Response of PtOEP fluorescence spot to 0% OW and air saturated water using Prototype 1. (A) 0% OW was manually injected at varying intervals for 1 min and (B) Start of constant flow of air saturated water.	23
Figure 2.3. Response of PtOEP fluorescence spot to 0% OW under constant flow rate and 90/30 s and 6/2 min flow/stop cycle using Prototype 1.	24
Figure 2.4. Response of PtOEP fluorescence spot to CRL 2303 cells from 90/30 s flow/stop cycle, 50% flow rate using Prototype 1.	25
Figure 2.5. Images of CRL 2303 at the bottom of the well plate: 1&2) before the measurement, 3&4) after the measurement.	26
Figure 2.6. Experimental set up for Prototype 2. Components are not to scale.	28
Figure 2.7. Response of PtOEP fluorescence film to 0% OW under constant flow rate and 90/30 s and 6/2 min flow/stop cycle using Prototype 2.	29
Figure 2.8. Illustration of “RedEye Oxygen Sensing Patches” from Ocean Optics.	29
Figure 2.9. Response of commercially available Ocean Optics fluorescence oxygen sensitive “Redeye” film to 0% OW under constant flow rate and 90/30 s and 6/2 min flow/stop cycle using Prototype 2.	30
Figure 2.10. Comparison of different fluorophore film response from (1) Prototype 1 with fluorophore spot, (2) Prototype 2 with PtOEP fluorophore film, (3) Prototype 2 with Ocean Optics fluorophore film using 0% OW under constant flow rate, 90/30 s (A) and 6/2 min (B) flow/stop cycles.	31

Figure 2.11. Response from <i>C. albicans</i> using Prototype 2 using first protocol using 90/30 s flow/stop cycle and 50% flow rate.....	32
Figure 2.12. Response from <i>C. albicans</i> using Prototype 2 using final protocol using 90/30 s flow/stop cycle and 50% flow rate.....	34
Figure 3.1. A) Oxygen during a flow cycle in transverse direction, B) Consumption of oxygen during a stop cycle. Components not to scale.	37
Figure 3.2. Image of various PtOEP sensor films on a cellulose tape.....	40
Figure 3.3. (A) Schematic of the experimental setup. (B) Face view of the modified Cytosensor [®] Microphysiometer sensor head showing the fiber optic bundle placement. (C) Cross-sectional side view of the sensor head in a well of a 24-well plate with a Transwell [®] cup.	41
Figure 3.4. PtOEP film fluorescence response to 0% oxygen DI water (A) and ambient oxygen DI water (B). The solution is switches every 3 min.....	43
Figure 3.5. PtOEP film fluorescence response to <i>C. albicans</i> oxygen consumption during YPD media perfusion using a 90/30 s flow/stop cycle. A longer stop cycle can be seen after 21 min.....	44
Figure 3.6. Response of PtOEP/cellulose film with <i>C. albicans</i> to varying flow/stop cycles (A) 45/15, (B) 40/20, (C) 90/30, (D) 75/45, (E) 60/60, (F) 90/90 s.....	45
Figure 3.7. Changes in PtOEP film fluorescence intensities (untreated data) with 90/30 s flow/stop cycles in response to 1) <i>C. albicans</i> with YPD media perfusion, 2) no cells with changing water temperature (initial = room temp, A = cool, B = warm), and 3) no cells with YPD media perfusion followed by YPD/NaF (C) and DI water (D).....	47
Figure 3.8. A) Raw fluorescence intensity data of <i>C. albicans</i> upon treatment with 50 mM NaF. B) Raw data peak heights normalized to baseline (100%). Each data point above 100% represents one 90/30 s flow/stop cycle.	49
Figure 3.9. Effect of different concentration of NaF 5 mM (126 to 136 min), 10 mM (136 to 146 min), 25mM (146 to 156 min), 50 mM (156 to 166 min), 100 mM (262 to 284 min) on the oxygen consumption rates of <i>C. albicans</i>	51

Figure 3.10. Raw data for glucose, lactate, and oxygen response to the addition of 0.5 mM DNP to CHO cells in the modified Microphysiometer. The pump cycle consisted of a 60-s flow and 30-s stop-flow phase [2].....	52
Figure 3.11. Effect of 4mM DNP (222 to 244 min) on the oxygen consumption of <i>C. albicans</i> . The decrease in the oxygen consumption of cells can be observed in the presence of DNP.....	53
Figure 3.12. Effect of increasing glucose concentrations (0.5% to 2%) on the oxygen consumption rate of <i>C. albicans</i> . Upon addition of YPD with 2% glucose, the rate of increasing fluorescence intensity increases by nearly 50%, indicating an increase in the oxygen consumption rate of the cells by nearly 50%.	54
Figure 4.1. <i>C. albicans</i> response to 50mM NaF from 188 to 210 min and 290 to 312 min using 90/30 s flow/stop cycle and 50% flow rate.....	61
Figure 4.2. <i>C. albicans</i> response to 2 µg/ml AMB (46 to 188 min) and 50mM NaF (338 to 360 min) using 90/30 s flow/stop cycle and 50% flow rate.	62
Figure 4.3. <i>C. albicans</i> response to 4 µg/ml AMB (50 to 282 min) and 50mM NaF (338 to 360 min) using 90/30 s flow/stop cycle and 50% flow rate.	63
Figure 4.4. <i>C. albicans</i> response to 8 µg/ml MCZ from 90 to 224 min and 50 mM NaF from 280 to 302 min using 90/30 s flow/stop cycle and 50% flow rate.....	65
Figure 4.5. <i>C. albicans</i> response to 8 µg/ml FCZ (72 to 314 min) and 50 mM NaF (334 to 356 min) using 90/30 s flow/stop cycle and 50% flow rate.....	66
Figure 4.6. <i>C. albicans</i> response to 16 µg/ml FCZ from 96 to 342 min, 50 mM NaF from 358 to 380 min, and 200 mM NaF from 398 to 420 min using 90/30 s flow/stop cycle and 50% flow rate.....	67
Figure 5.1. (A) Image of the sensor head 3D design from Tinkercad software, (B) 3D printed sensor head with fiber optic bundle and solution perfusion tubes.	69

Figure 5.2. PtOEP film fluorescence response to <i>C. albicans</i> oxygen consumption during YPD media perfusion using a 90/30 s flow/stop cycle using the 3D printed sensor head.	70
Figure 5.3. Effect of 200 mM NaF on the oxygen consumption of <i>C. albicans</i> during YPD media perfusion using a 90/30 s flow/stop cycle using the 3D printed sensor head.	71

ACKNOWLEDGMENTS

I gratefully acknowledge Dr. Sven E. Eklund for his supervision and guidance during this work.

I would like to thank Dr. Patrick Hindmarsh for his guidance during *C. albicans* culture protocol development and, also Hunter Collins for his help during that process. I would also like to thank William Johnston for his suggestions and help in writing this dissertation.

I am grateful to all the staff in the Chemistry and Biomedical departments. Special thanks are due to my friends for being my surrogate family during the years I stayed with them and for their continued moral support thereafter.

Finally, I am forever indebted to my family members for their understanding and encouragement when they were most required.

1.0 INTRODCUTION

1.1 Motivation

Cell metabolic studies are an important aspect of basic biology and drug discovery. They can provide a better understanding of cellular growth, function, and response to physiological agents. Metabolic studies generally measure changes in the rate of cellular consumption/production of various metabolic analytes such as oxygen, glucose, lactate and H^+ . In this respect, *in vitro* studies of cells show consumption and release of various analytes into the extracellular environment during normal cell function or in response to external stimuli. Concentration changes of analytes in the extracellular environment can indicate intracellular metabolic activity. Many common methods of studying cell cultures operate on a time scale of hours or days and generate incremental data. A tool that can measure multiple analytes in the extracellular environment in real-time would aid researchers in the study of metabolic pathways. Presently, few available tools [1][2][3] give researchers this ability. To address this challenge, a new sensor for measuring real-time changes in extracellular oxygen concentration in a traditional well plate using a fluorescent sensor has been developed. The design of this sensor and platform is versatile enough to incorporate multiple other fluorescent sensors and can be adapted to fit any traditionally available well-plate size.

1.2 Cell Metabolic Measurements

Cell metabolism is a complex process where cells consume and produce various analytes in the intracellular and extracellular environments as part of their normal life cycle, and in response to various metabolic and external stimuli. Metabolism is generally divided into two processes: catabolism and anabolism. Catabolism is the breakdown of macro molecules to produce energy from the organic substances available to cells. Anabolism uses this energy to produce cellular components such as proteins and nucleic acids, which are required for cell function. The chemical transformations of these compounds are known as metabolic pathways, which involve various enzymes and cofactors. A simplified cell model, shown in Figure 1.1, illustrates a metabolic pathway for extracellular concentrations of analytes resulting from intracellular consumption of glucose and oxygen and production of lactate and carbon dioxide (which contribute to changes in extracellular H^+ concentration).

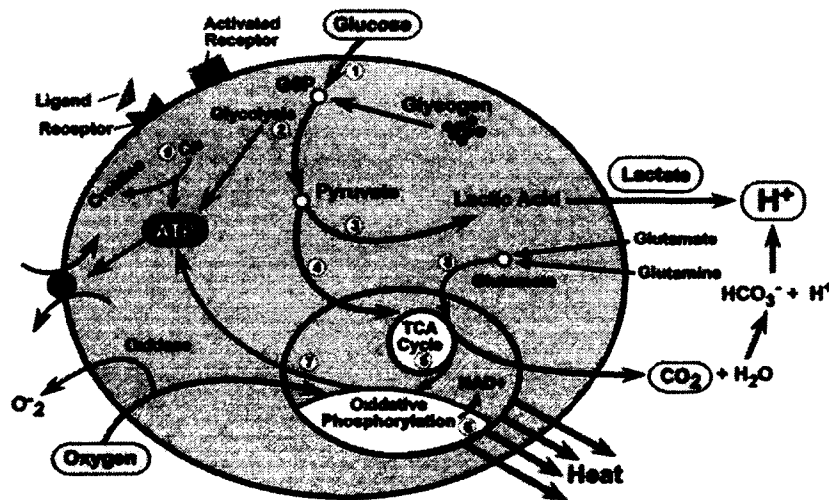


Figure 1.1. Simplified extra- and intracellular metabolic cell model highlighting glycolysis [4].

If changes in concentration of analytes in the extracellular environment can be measured, they would be an indicator of cellular metabolic rates. In a static environment, the extracellular media is not refreshed. A sensor could determine the consumption of resources and production of waste products, but the continuous increase of these analytes would affect the metabolism. In an open flow system, analytes in the extracellular media are replenished and waste products are continuously removed. When the cells are stimulated with a metabolic agent, the changes in the rate of appearance (production) or disappearance (consumption) of extracellular analytes would be an indicator of changes in cell metabolism. Some of the most common analytes measured as indicators of cellular metabolism are oxygen, glucose, calcium, lactate, and pH [5].

In recent years, efforts have increased to develop technologies for measuring the concentration changes of analytes involved in cellular metabolism [1][3][6][7]. These measurement techniques have been applied to further understanding in the fields of metabolomics, systems biology, and pharmacology. Many types of sensors have been designed to measure analytes that are indicators of metabolic activity in the extracellular environment [7][8][9][10][11][12] and the obtained information is used to characterize cellular metabolic pathways. Traditional metabolic analysis studies also use large numbers of cells and the experiments are done on the time scales of hours and days. Any improvements over the traditional methods can be helpful for researchers in studying cellular metabolism.

1.3 Cytosensor® Microphysiometer

Many research groups have developed sensors to monitor the extracellular analyte flux as an indicator of cellular metabolism [5][6][10][9][13][12]. In this respect, the Cytosensor® Microphysiometer was initially developed to measure acidification rates in the extracellular environment using a light-addressable potentiometric sensor (LAPS) [12][14][15][16]. It required smaller samples of cells compared to traditional methods [1]. The Microphysiometer used an electrochemical sensor known as a light-addressable potentiometric sensor (LAPS) for measuring changes in the acidification rate of the extracellular environment. A descriptive image of the Cytosensor® Microphysiometer pH sensor setup can be seen in Figure 1.2.

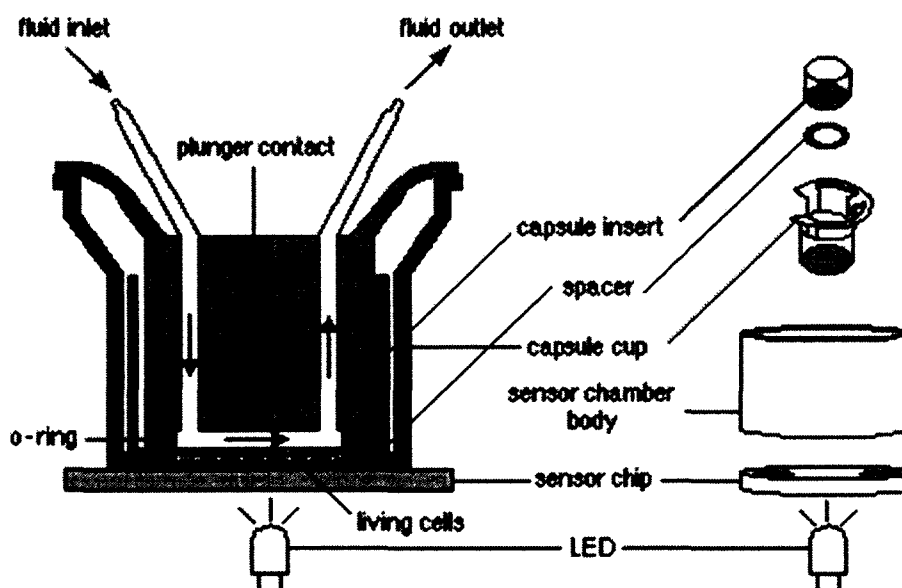


Figure 1.2. Cytosensor® Microphysiometer pH sensor cell setup [17].

The Cytosensor® works by positioning the LAPS a few microns below cells that are sandwiched between specialized cups with porous membranes. The porous membranes allow changes in extracellular pH to be detected at the LAPS. The

Microphysiometer is designed around transverse laminar flow/stop cycles where buffered media is perfused above the top porous membrane (typically for 90 s), and then perfusion is stopped (typically for 30 s). When the media flow is stopped, cellular metabolites produced or consumed by the cells cause a change in pH in the confined space of the media near the sensor. These changes in pH are detected by the LAPS sensor and are proportional to cellular metabolic rates. At the end of the 30 s stop, another 90/30 s flow/stop cycle is continued, producing a series of sloping lines during the stop portion of the cycles shown in Figure 1.3.

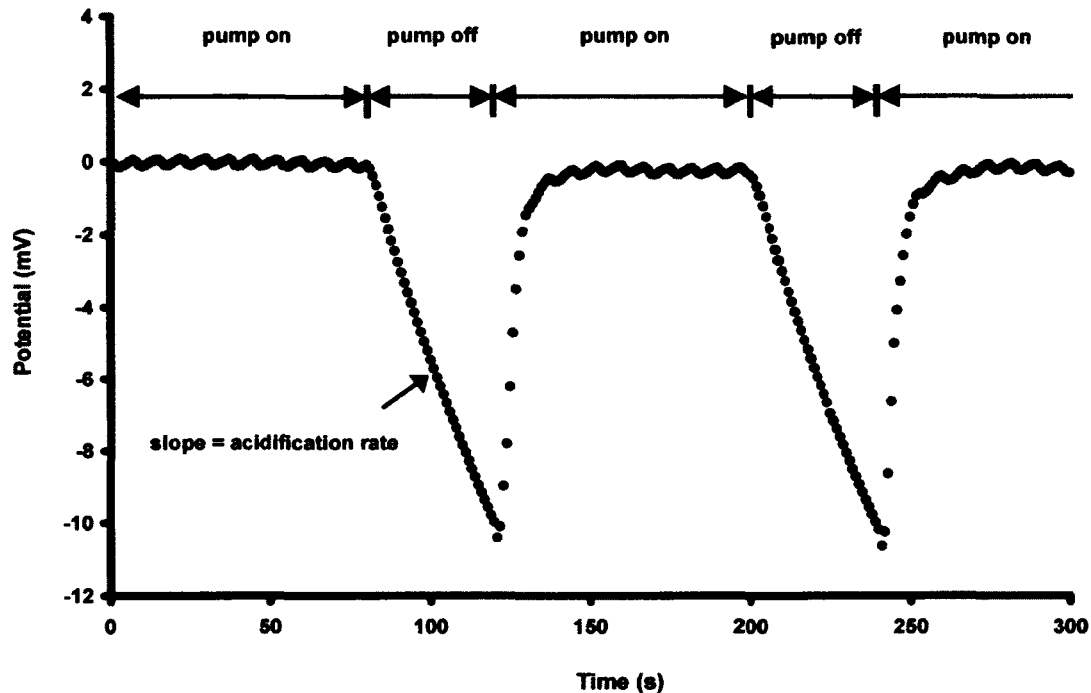


Figure 1.3. Acidification rate measurements using the Cytosensor[®] Microphysiometer [2].

Measuring the slope of the signal change during each stop cycle is an indicator of the change in the extracellular acidification rate (ECAR). Use of the slope also minimizes affects from baseline drift during flow. Once the basal metabolic rate has been

established after several flow/stop cycles, a metabolic agent can be introduced and the change in the slope observed.

The Cytosensor[®] Microphysiometer led to a number of cellular studies [16][18][19][20][21] where the change in extracellular pH was related to metabolic changes in the cells. Unfortunately, this technique only provides single-analyte measurements. Other researchers have worked to modify the equipment for multiple analyte measurements. Jung et al. modified the Cytosensor[®] to measure the changes in glucose and oxygen in the extracellular environment with respect to the intracellular change in Ca²⁺ concentrations of pancreas islets [8]. Eklund et al. [2][4][22] modified the Cytosensor[®] (Figure 1.4) to concurrently measure changes in glucose, oxygen, lactate and pH using electrochemical-based sensors at platinum electrodes.

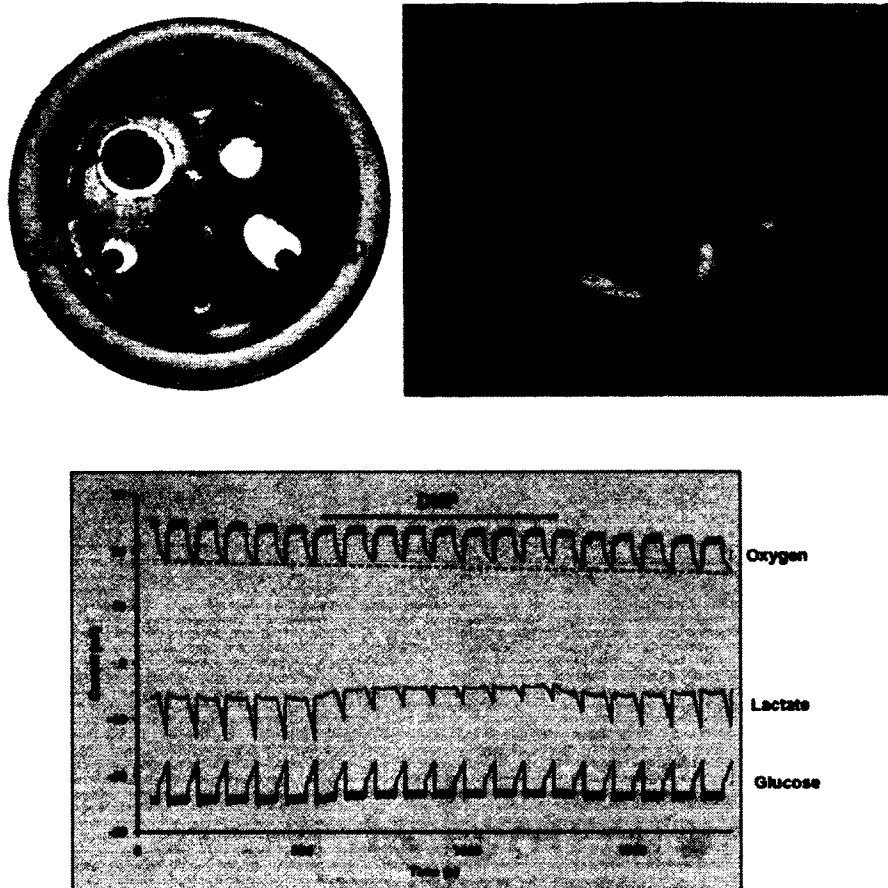


Figure 1.4. Top left: modified Cytosensor[®] Microphysiometer sensor head with four (A, B, C, D) platinum electrodes. Top right: the electrochemical measurement setup. Bottom: changes in oxygen and glucose consumption and lactate production rates of CHO cells in respiration [2].

The Cytosensor[®] Microphysiometer platform is no longer commercially available, including the specialized apparatus for cell handling. In a step towards miniaturizing the Cytosensor[®] Microphysiometer technology into a compact microfluidic device, Lima et al. [23] have developed a multi-potentiostat system that uses amperometry and potentiometry-based measurements for detecting changes in multiple analytes. Even with these advancements with electrochemical sensors, some disadvantages still exist. Most electrochemical sensors consume analyte during the measurement process, are temperature sensitive, have a short shelf life, and require specialized circuits for

separating noise from signal when working at the nano ampere (nA) current range, which complicates data collection and interpretation [24]. In addition, many biotechnology lab technicians have little to no experience working with electrochemical apparatus.

These disadvantages can be overcome by using fluorescence-based sensors to measure the analyte concentration changes. Similar to electrochemical sensors, fluorescence-based measurements have rapid response times, low detection limits, and are unaffected by small temperature changes. The additional advantage of fluorescent sensors is they do not typically consume analyte during the measurement process [24][25], potentially do not harm cells, and biology researchers are more familiar with fluorescence than electrochemical techniques.

Fluorescence-based sensing has been a growing area of research for the past three decades and has become a powerful analytical and diagnostic tool [25]. Fluorescence-based sensors have been applied to the fields of biotechnology, drug discovery, and medical and environmental testing. Among many other applications, these biosensors have been used to measure cell metabolic changes [3], detect toxic molecules in the gas phase[26], measure small glucose concentrations for treating diabetic patients [27], and measure ammonia levels in sea water during environmental studies [28].

Our area of interest is in performing cell metabolic studies using fluorescence-based sensors, but presently most of the fluorescence-based biosensors either have the fluorophore in the cells or in the extracellular environment [24][29]. The fluorescence is imaged with a fluorescence microscope or spectrometer. Since the cells in this type of measurement format are physically exposed to the fluorophore, there might be an effect of the fluorophore on the cells themselves, or the effect of the cells on the fluorophore

due to protein binding, for example. PEBBLE sensors (Probes Encapsulated By Biologically Localized Embedding) [30][31] were developed to overcome these disadvantages by entrapping the fluorophore in an inert sol-gel matrix followed by introduction into the cells. The protective sol-gel coating eliminates interferences from protein binding and/or membrane/organelle sequestration, which can alter the fluorophore response. However, injection of the sol-gel PEBBLES into the cells requires specialized instrumentation, and it is unclear at this time whether the injection step or unknown nanoparticle toxicity adversely affects the cells. The PEBBLE sensors also only measure the intracellular analyte changes with time.

To overcome the disadvantages, we have developed a fluorescence-based sensor platform that can monitor changes in extracellular analytes in real-time. A fluorophore embedded in a thin film affixed to a fiber optic in the extracellular environment was developed so the cells would not be directly exposed to the fluorophore. The sensor was designed to fit in a traditional 24-well plate familiar to biotechnology researchers. Yeast cells (*Candida albicans*) in combination with an oxygen sensor were used as a test platform for proof of concept.

1.4 Fluorescence Spectroscopy

Fluorescence spectroscopy is a well-studied technique used in areas of research spanning biology to physics. Fluorescence occurs when a molecule absorbs light from an excitation source and emits at longer, lower energy wavelengths. Molecules that emit the absorbed energy in the form of fluorescence are called fluorophores. A Jablonski diagram can be used to illustrate the excitation and emission changes of a fluorophore. As shown in Figure 1.5, when a fluorophore absorbs the excitation wavelength from a light source,

the electrons are transferred to higher energy orbitals (S_1 , S_2) from their ground state (S_0). These orbitals consist of electronic, vibrational, and rotational energies. Normally this excited state energy is dissipated as vibrations or heat by molecular collisions and is called internal conversion. In some molecules, electrons can first lose vibrational and rotational energy by internal conversion to an electronic energy level, then return to their ground state (S_0) by emission of a photon. This photon will be at lower energy than the absorbed photon from loss of the rotational and vibrational energy.

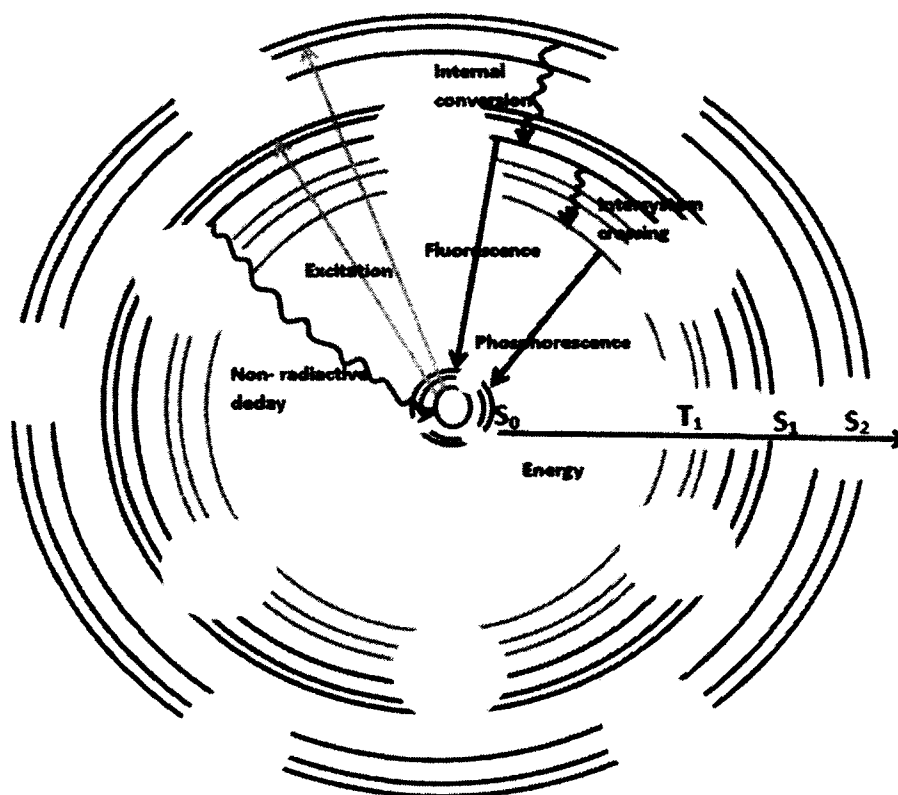
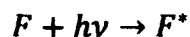


Figure 1.5. Jablonski diagram [32].

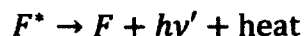
The lifetime of fluorescence is generally in nanoseconds and is a cyclical process. Emission after intersystem crossing has occurred is called phosphorescence and occurs at an even lower energy and at longer times, milliseconds to seconds, than fluorescence.

Interaction between a fluorophore (F), excited state fluorophore (F^*), excitation wavelength energy ($h\nu$), and emission wavelength energy ($h\nu'$) can be stated:



Excitation

Equation 1.1



Emission at a longer wavelength.

Equation 1.2

Any given fluorophore has an excitation and emission spectrum where the excitation wavelengths are shorter (higher energy) than the emission wavelengths. An excitation/emission spectrum is generally represented as a graph of excitation/emission intensity (y-axis) vs. wavelength (x-axis) as depicted in Figure 1.6. The emission intensity of any fluorophore is directly proportional to the incident excitation energy. Typically, excitation of a fluorophore is performed at its maximum intensity excitation wavelength for maximum fluorescence quantum yield. However, the fluorophore can be excited at any wavelength that it will absorb and produce the same fluorescence emission spectrum, although at reduced intensity. The difference in the peak wavelengths (λ) of the excitation and emission intensities is called the Stokes shift. Generally, fluorophores with larger Stokes shifts are desirable because the emission spectrum can be more easily separated from the absorption spectrum.

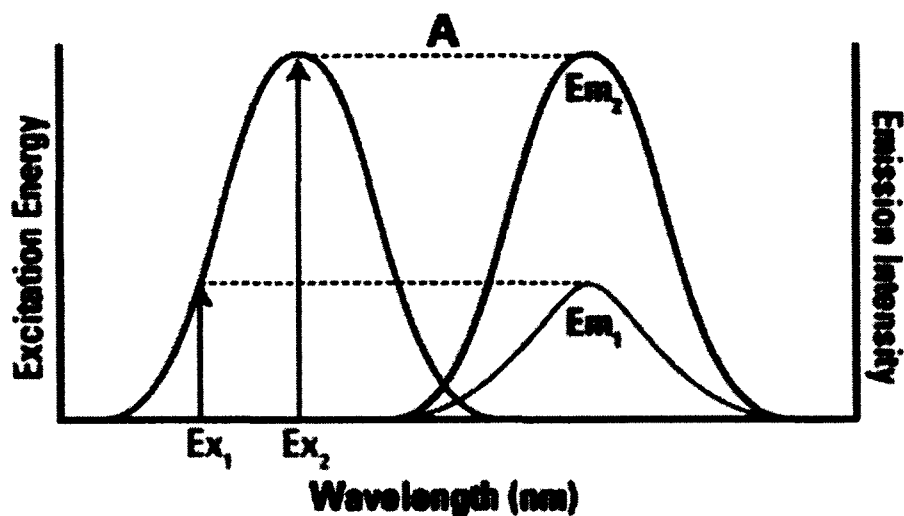


Figure 1.6. Excitation spectrum of a fluorophore and the resulting fluorescence emission spectra at different excitation wavelengths [33].

1.5 Fluorescence Instrumentation

Instruments used to measure fluorescence are called spectrofluorometers. A typical spectrofluorometer consists of a light source, monochromator(s), sample cell, and detector. Energy from an excitation light source passes through a monochromator and excites the sample. This sample emits fluorescence in all directions, but is typically collected at 90° angles to minimize light from the excitation source. A schematic of a fluorescence measurement setup is shown in Figure 1.7.

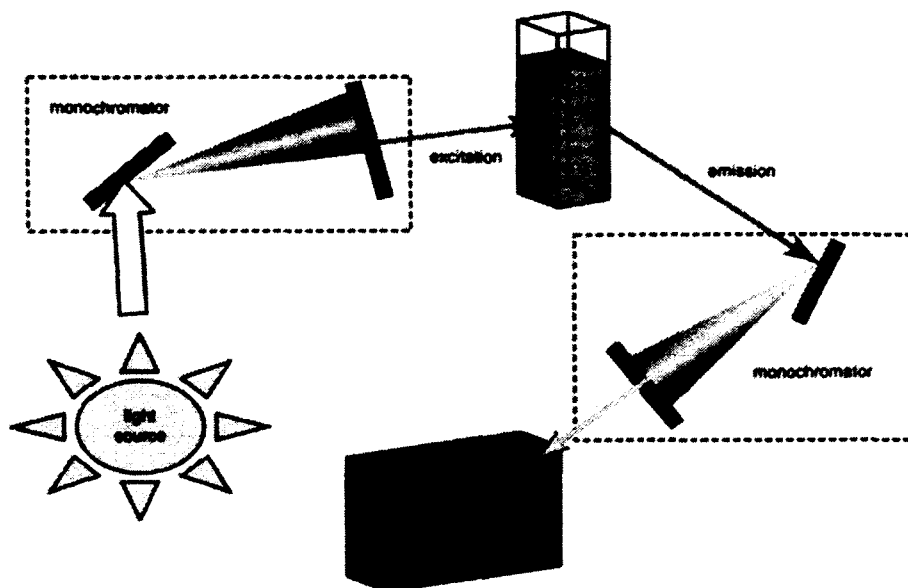


Figure 1.7. General schematic of a spectrofluorometer [34].

A wide variety of light sources are used in spectrofluorometers, the majority consisting of xenon lamps, mercury-vapor lamps, LEDs, and laser diodes. Xenon lamps are the most common light source used because of their capability to emit continuous light for wavelengths ranging from 250 to 700 nm. If a specific excitation wavelength is required for an experiment LEDs can be a good alternative and research is being carried out to develop white LEDs capable of emitting wavelengths comparable to traditional xenon lamps. LEDs have advantages like low power consumption, low cost, and longer lifetimes compared to other light sources [25]. Other light sources like mercury-vapor lamps are used if a narrow bandwidth light source is required and lasers diodes are used for pulsed or modulated excitation wavelengths.

Different types of detectors are also currently available to collect the fluorescence emission from the sample. The main types of detectors used in spectrofluorometers are photo multiplier tubes (PMTs), charge-coupled devices (CCDs), and photovoltaic cells. A PMT is used in most commercial spectrofluorometers and is capable of detecting single

photons under ideal conditions. CCDs are becoming a more popular alternative to PMT because of their smaller footprint, lower cost, and more rapid data acquisition [25].

Combined application of these advancements has led to the miniaturization of spectrofluorometers, which use LEDs as a light source and CCDs as detectors. An example of these instruments are the Ocean Optics miniature spectrophotometers, which have no moving parts (Figure 1.8), collect the entire spectral range of the monochromator in fractions of a second, and are designed to be modular, so different wavelength sources can be attached and two or more spectrometers can be connected to work in tandem. They typically use fiber optic cables for transmission of the excitation/emission wavelengths. The portability of these spectrofluorometers has helped researchers to envision and implement new experimental designs which were not possible before.

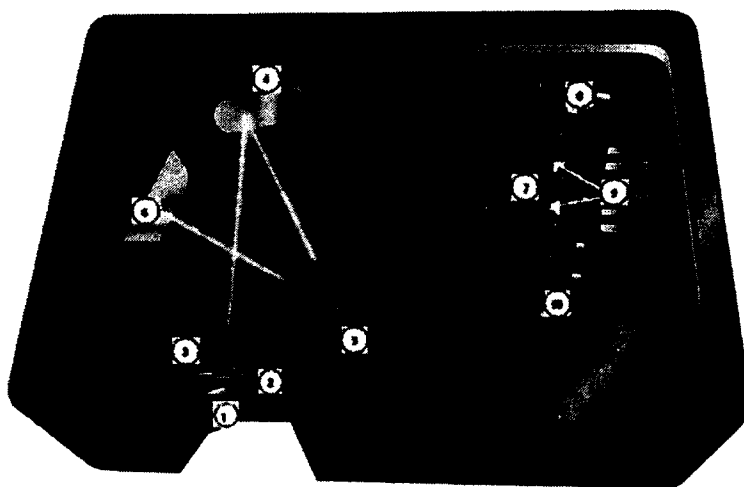


Figure 1.8. Portable USB4000 FL Spectrometer and its Components. 1) SMA 905 Connector 2) Entrance slit 3) Filter 4) Collimating Filter 5) Grating 6) Focusing Mirror 7) Detector Collection Lens 8) Detector 9) Filter 10) Detector. Dimensions of an Ocean Optics 4000 FL Spectrometer are 89.1 mm x 63.3 mm x 34.4 mm [35].

1.6 Fluorophores for Detecting Oxygen

Oxygen was chosen as the test analyte because it is one of the most important and significant components of cellular metabolism. Cells consume oxygen present in the extracellular environment to perform metabolic functions, like cellular proliferation and growth. Monitoring oxygen concentration changes in the extracellular environment would be a useful tool in understanding cellular behavior and response to metabolites in the extracellular environment. Due to the importance of oxygen in the cellular environment, developing optical sensors for detecting oxygen concentration changes is an active research area [36].

One of the earliest oxygen sensors developed, and still in use in many modified ways today, is the Clark electrode [37], which is an electrochemical sensor where reduction of oxygen is measured as current flow by the electrodes. A schematic of a Clark electrode is shown in Figure 1.9.

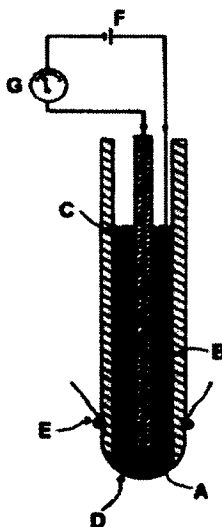


Figure 1.9. Clark electrode: (A) Pt-electrode, (B) Ag/AgCl-reference, (C) KCl electrolyte, (D) Teflon membrane, (E) rubber ring, (F) voltage supply, (G) galvanometer [37].

Researchers have worked towards miniaturizing oxygen sensors like the Clark electrode and other electrochemical sensors for detecting oxygen concentration changes in the extracellular environment. Despite the miniaturization of electrochemical sensors some disadvantages still exist, like analyte consumption, easy contamination by sample components, and requirement of continuous sample stirring for accurate measurements [24]. Optical sensors using fluorophores are becoming a good alternative to overcome these disadvantages.

Currently available oxygen sensitive fluorophores include those based on polycyclic aromatic hydrocarbons, transition metal polypyridyl complexes, metal-porphyrins, and cyclometallated complexes [38][39][40]. Of these, metal-porphyrins like platinum-octaethylporphyrin (PtOEP) and palladium-octaethylporphyrin (PdOEP) are the most commonly used and studied because of their large Stokes shift, strong room temperature fluorescence, and longer fluorescence lifetime than other fluorophores [41]. Metal-porphyrins are macrocyclic structures containing four pyrrole rings with a metal bound equally to the nitrogen atoms of the pyrrole rings, as seen in Figure 1.10. The Pt atom at the center of the porphyrin molecule provides rigidity to the structure, decreasing the amount of molecular movement and thermal relaxation, thus promoting more fluorescence emission.

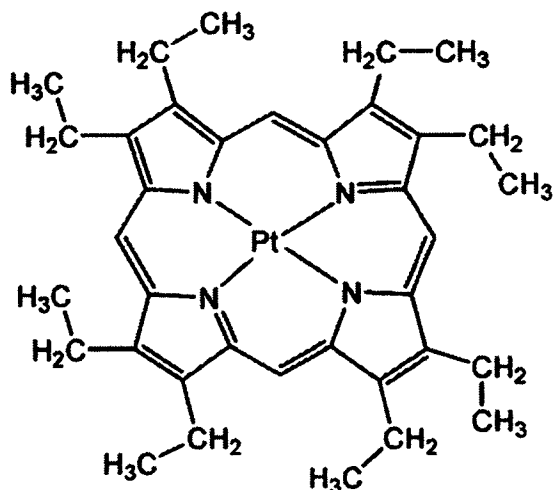


Figure 1.10. Structure of platinum-octaethylporphyrin (PtOEP) [42].

Metal-porphyrins like PtOEP and PdOEP have been embedded in different encapsulating media, like polystyrene, polypropylene, and cellulose acetate to form films for use in different fluorescence-based oxygen sensors [41][43]. As seen in Figure 1.11 [43], PtOEP embedded in a polymer film can recover faster than PdOEP when switching between 100% argon and 100% oxygen conditions. Fast recovery time was an important factor to consider for the flow/stop cycle measurements performed in this dissertation.

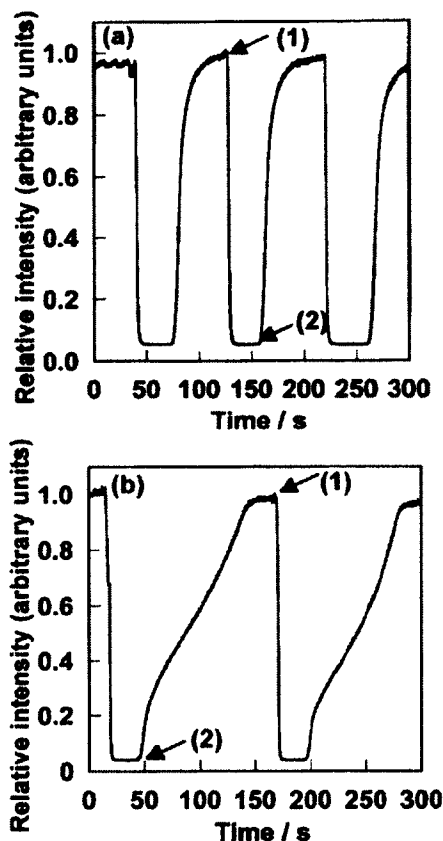


Figure 1.11. Response times and relative intensity changes for (a) PtOEP and (b) PdOEP immobilized in poly-Sty1-co-PFS0.21 film on switching between 100% argon (1) and 100% oxygen (2) for 300 s. The excitation wavelengths for PtOEP and PdOEP were 535 and 546 nm, respectively, and the emission wavelengths were 645.4 and 663.8 nm, respectively [43].

Many of the oxygen sensitive fluorophore films are prepared on glass or polymer surfaces [29][44][45][46], and an adhesive is required for attaching the glass slide to the fiber optics in the sensor head. Our design uses a thin film ($\sim 35\mu\text{m}$) with an adhesive on one side so that it can be attached/detached easily from the fiber optics embedded in the sensor head.

This dissertation explores the development of a fluorescence-based measurement platform using fiber-optics for transmission of the excitation and emission wavelengths of a new PtOEP fluorescent oxygen sensor that makes use of a commercially available

cellulose acetate film. The robustness of the new oxygen sensing film is determined by exposure to temperature changes and various flow solutions conditions and analytes. To show the applicability of this platform and sensor to real-time metabolic studies of cultured cells, changes in oxygen consumption rates of *Candida albicans* was monitored before and after exposure to antifungals, followed by post treatment with fluoride, in an effort to reveal synergistic activities between the metabolic agents.

2.0 PLATFORM DESIGN

2.1 Introduction

In this chapter, two experimental platform designs are presented and discussed. A commercial and two in-house oxygen sensors were tested in each platform. The technique developed for plating of the cells in the well plate will also be discussed.

2.2 Platform 1

The initial scheme for measuring changes in cell metabolism by monitoring changes in multiple analyte consumption/production rates used an array of sensors in a transverse flow environment. In this scheme, the perfusion media solution was allowed to flow across the center of a sensor head that fits in a standard well-plate. The sensors were embedded in and positioned radially from the center of the sensor head. The first Prototype is illustrated in Figure 2.1, showing a sensor head with one fiber optic bundle in the radial position, and a fluorophore on the bottom surface of the disposable cup.

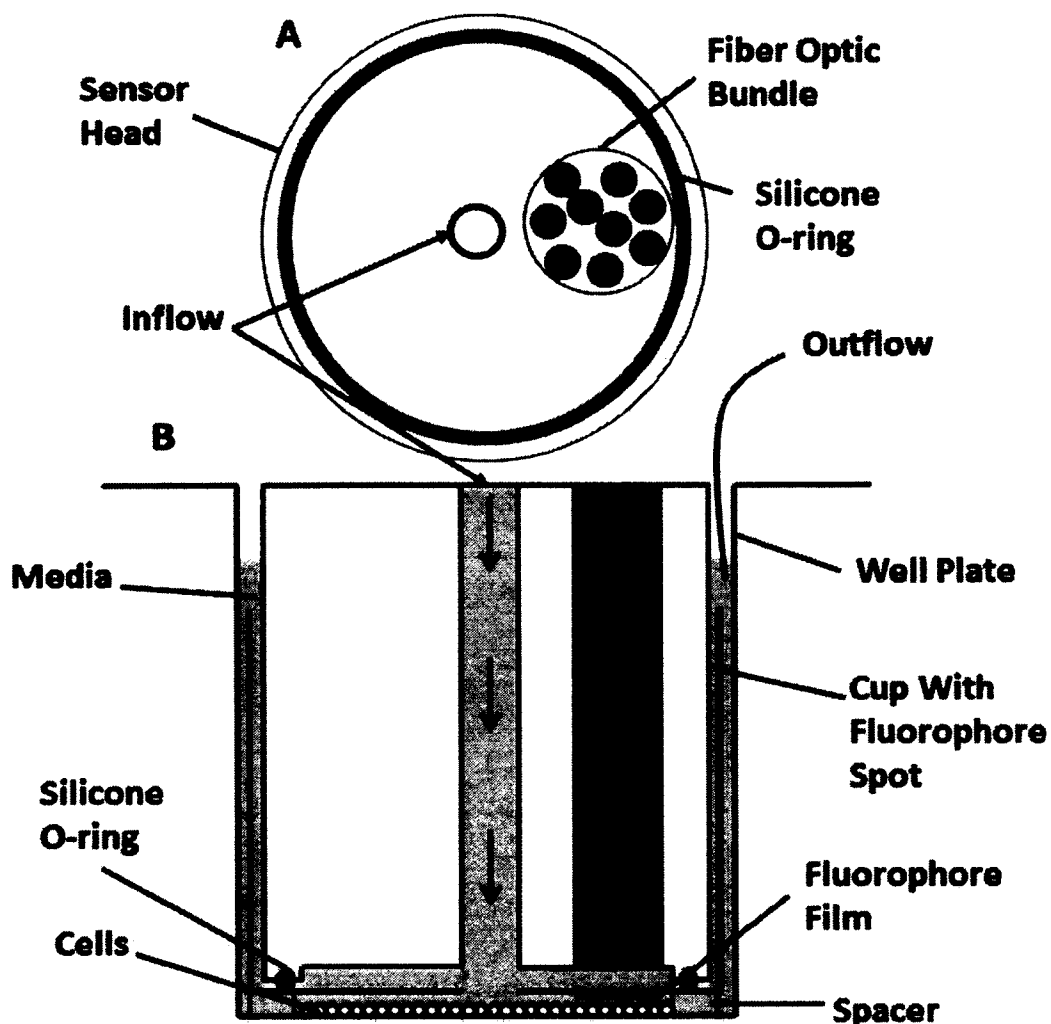


Figure 2.1. Experimental set up for Prototype 1. Components are not to scale.

A sensor head from the Cytosensor[®] Microphysiometer was modified to implement the first Prototype scheme. A hole was drilled in the center of the sensor head and a 2 mm diameter hard plastic tube was set in place using epoxy. Another hole was drilled in a radial position, a fiber optic bundle inserted, and set in place with epoxy. To make the film, 0.3 mg of PtOEP were dissolved in 0.5 ml of acetone, and 3 μ l of this solution was dropcast, in the same radial position as the fiber bundle, on a 12 mm diameter cup with a 2 mm hole in the center. As the acetone evaporated, PtOEP was

embedded in the surface of the cup, making a thin film that was sensitive to changes in oxygen concentration. To allow for radial flow of the solution from the bottom of the cup and prevent crushing the cells during insertion of the cup into the well small "feet" on the cup were created by placing four spots of epoxy on its edge and polishing them with fine sandpaper so their height ($\sim 500 \mu\text{m}$) was even across all the spots.

For the metabolic measurement protocol, cells were first seeded in the bottom of a well plate. The cup with a fluorophore spot on the bottom was then inserted into the well. These feet at the bottom of the cup supported it $\sim 500 \mu\text{m}$ above the cells. The sensor head was then inserted into the cup where it was sealed with an o-ring on the face against the cup so the solution would flow down the sensor head, through a hole in the cup, and into the well across the cells in a radial pattern. The fiber optic bundle was positioned directly above the fluorophore spot on the underside of the cup. The fluorophore spot was thin enough to not come in contact with the cells. The solution was pumped through the center of the sensor head using a peristaltic pump causing it to flow in a radial pattern across the cells at the bottom of the well, providing an even distribution of the flow. A small siphon tube was inserted in the side of the well to remove excess solution as it built up during flow.

2.2.1 Prototype 1 Response to 0% Oxygen Water

Prototype 1 was first used to test the response of the fluorophore spot to 0% oxygen water (0% OW). Since oxygen quenches PtOEP fluorescence, a decrease in oxygen concentration should lead to an increase in fluorescence intensity. N_2 gas was bubbled through DI water in a syringe pump for 30 min to remove dissolved oxygen. This 0% OW was manually injected 6 times from the syringe pump. The resulting

intensity vs. time plot can be seen in Figure 2.2. Immediately after the introduction of 0% OW, the fluorescence intensity sharply increased, then tapered off and reached a plateau after ~1 min. This decrease in fluorescence intensity can be attributed to the oxygen concentration of water in the well plate reestablishing equilibrium with atmospheric oxygen. Air-saturated water was introduced at ~40 min using a peristaltic pump to maintain a constant flow rate. At this point the fluorescence intensity decreased back toward the starting fluorescence intensity.

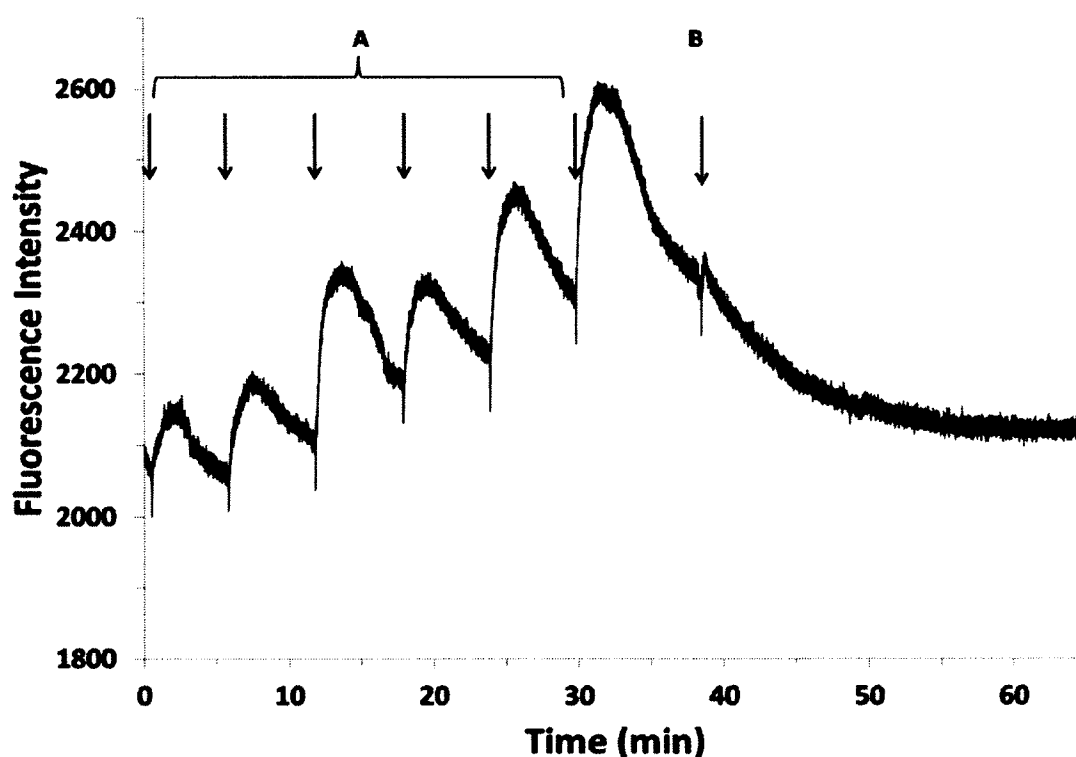


Figure 2.2. Response of PtOEP fluorescence spot to 0% OW and air saturated water using Prototype 1. (A) 0% OW was manually injected at varying intervals for 1min and (B) Start of constant flow of air saturated water.

As the measurement platform is based on flow/stop cycles and the response from the sensor during the stop cycles is important, Prototype 1 was tested under two different flow/stop conditions. First, 0% OW was pumped across the fluorophore spot at a constant

rate of 0.15 ml/min (50% of the peristaltic pump capacity). The data can be seen in Figure 2.3. After the fluorescence intensity reached a steady state, 90/30 s and 6/2 min flow/stop cycles were implemented. The response from the fluorophore spot during the 90/30 s flow/stop cycle was not very distinguishable from the baseline fluorescence intensity, and although the response from the 6/2 min cycles was comparatively better, it still exhibited a good bit of noise.

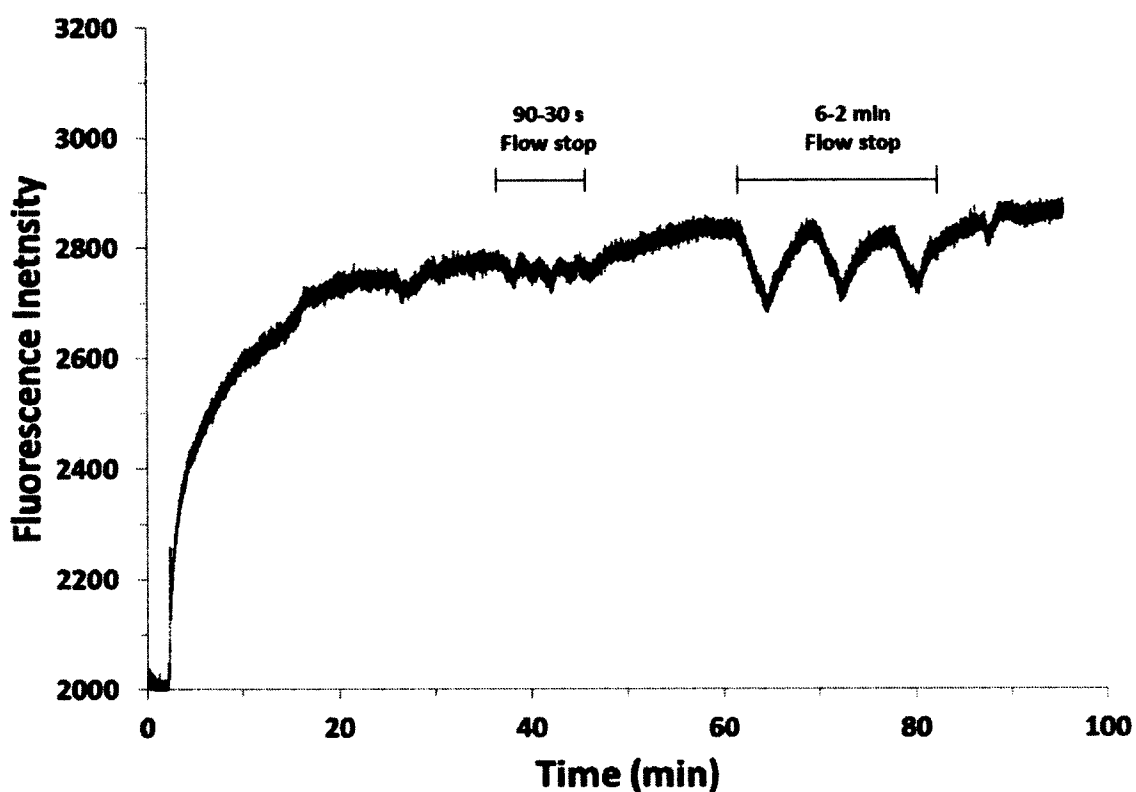


Figure 2.3. Response of PtOEP fluorescence spot to 0% OW under constant flow rate and 90/30 s and 6/2 min flow/stop cycle using Prototype 1.

The Prototype 1 sensor head was used in a cellular environment to help determine if this measurement scheme can be used to detect changes in the extracellular concentration of oxygen. CRL 2303 cells (provided by Dr. DeCoster's Lab at Louisiana Tech) were plated at the bottom of a 24-well plate and 2 ml of Locke's culture media was

added. The well plate was then kept in a 37°C incubator overnight and the final cell density was observed to be $\sim 5 \times 10^5$ per well. A constant flow rate and a 90/30 s flow/stop cycle were used to measure the response from the cells. The fluorescence data from this measurement are shown in Figure 2.4. The fluorescence intensity signal was not consistent initially and no significant change can be observed during the stop cycle.

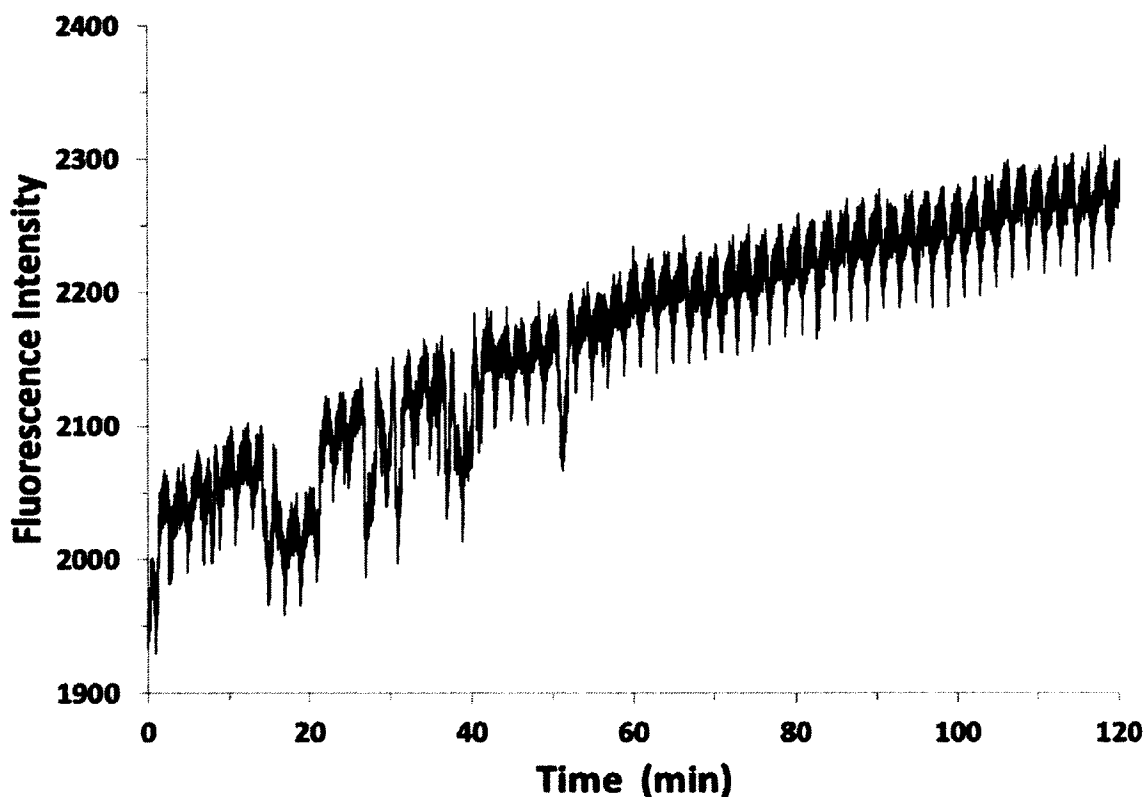


Figure 2.4. Response of PtOEP fluorescence spot to CRL 2303 cells from 90/30 s flow/stop cycle, 50% flow rate using Prototype 1.

To better understand these data, images of the cell culture before and after the experiment are shown in Figure 2.5. As can be seen in panels 1 and 2, before the measurement, CRL 2303 cells were spread evenly across the bottom of the well plate. After the experiment, Figure panels 3 and 4, the cells were unevenly deposited on the

plate, and no new cell growth was apparent, indicating that cells had washed off during the procedure.

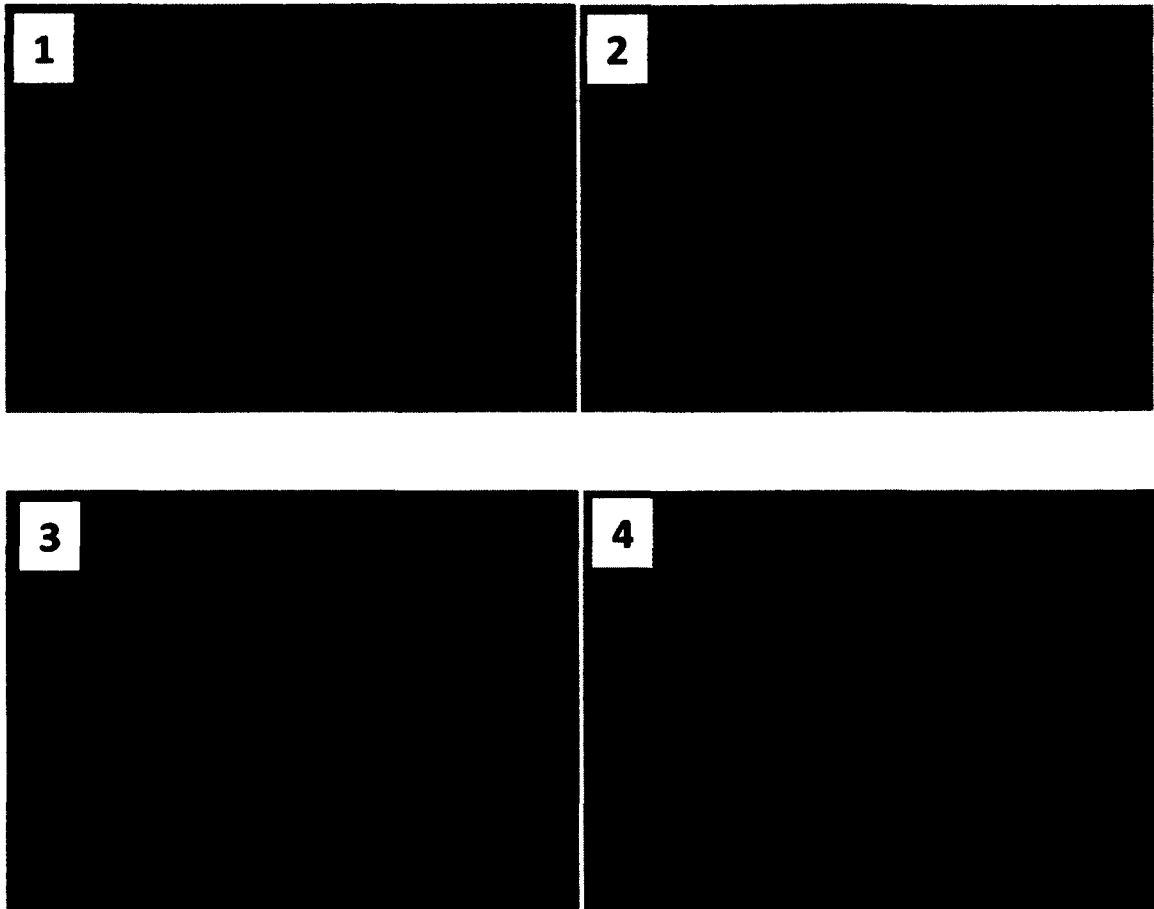


Figure 2.5. Images of CRL 2303 at the bottom of the well plate: 1&2) before the measurement, 3&4) after the measurement.

The fluorescence data and the images from the well plate suggest that the initial disturbance in the fluorescence intensity could be due to the cell wash off. The conditions provided during the experiment also may not have been conducive for the growth of CRL 2303 cells. After data from other experiments on Prototype 1 were analyzed, the design was modified to control cell wash-off at the bottom of the well plate, reduce distance

from the sensor spot and fiber optics, and reduce the distance between the cells and the sensor spot.

2.3 Platform 2

The previously discussed improvements were implemented during the development of second Prototype scheme to measure oxygen concentration changes in a 24-well plate. The new scheme is illustrated in Figure 2.6. A thin fluorophore film, which can be attached directly to the fiber optics, was developed instead of drop casting a fluorophore spot on a cup. After cells were plated in the 24-well plate, a Transwell[®] cup (3 μm pore size) with a 127 μm Parafilm[®] spacer was inserted in the well plate. A sensor head with the thin fluorophore film attached was inserted into the well plate making a seal between the sensor head and the cells. The solution was pumped through the sensor head using a peristaltic pump in a transverse pattern across the cells at the bottom of the well plate. This design was chosen for two main reasons. First, the flow approximates a laminar flow between the sensor and porous film. This flow creates an analyte barrier between the sensor and the extracellular environment, such that the sensor detects the oxygen concentration of the flow solution, which should remain constant, providing a baseline for oxygen concentration measurements. Second, the porous membrane prevents shear forces during flow from washing the attached cells from the well plate.

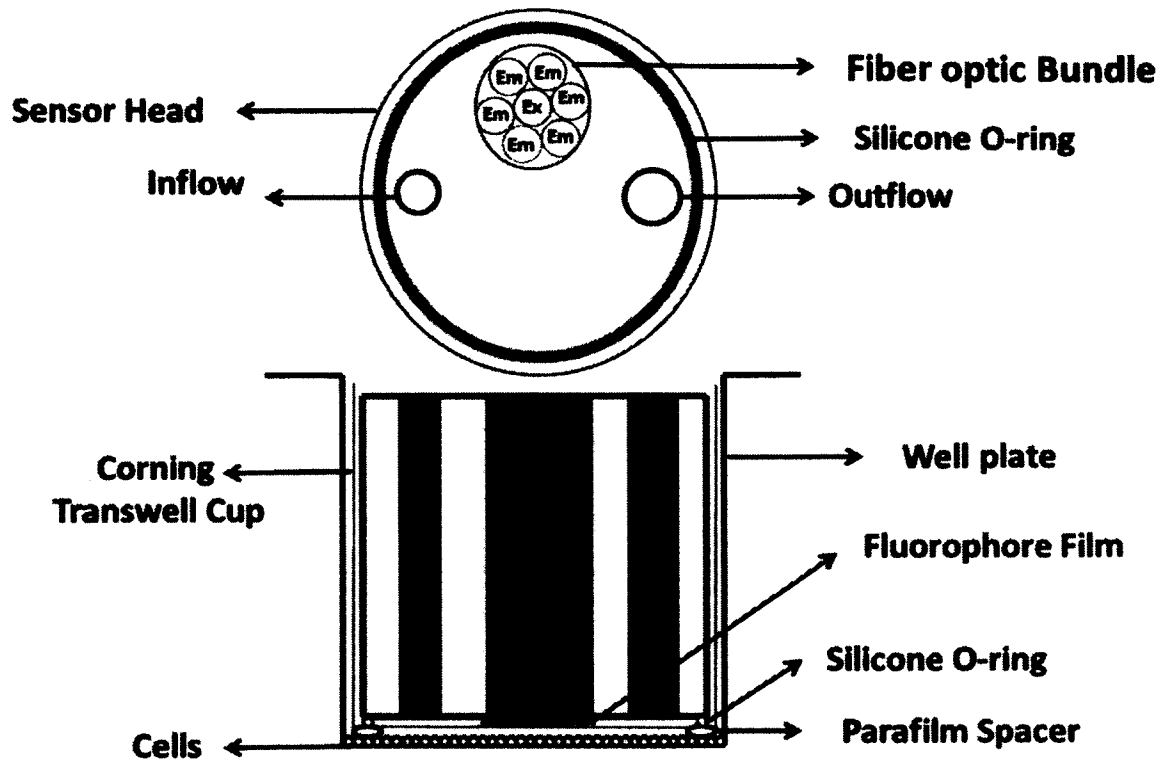


Figure 2.6. Experimental setup for Prototype 2. Components are not to scale.

2.3.1 Prototype 2 Response to 0% Oxygen Water

Prototype 2 was first tested by measuring oxygen concentration changes from 0% OW pumped across the fluorophore film. The same conditions used for testing Prototype 1 were implemented, which includes a constant flow rate of 0.15 ml/min, 90/30 s, and 6/2 min flow/stop cycles and the resulting data is shown in Figure 2.7. It can be seen in the figure that the response of the fluorophore spot during both the flow/stop cycles had a lower signal-to-noise compared to the data obtained using Prototype 1 (Figure 2.3).

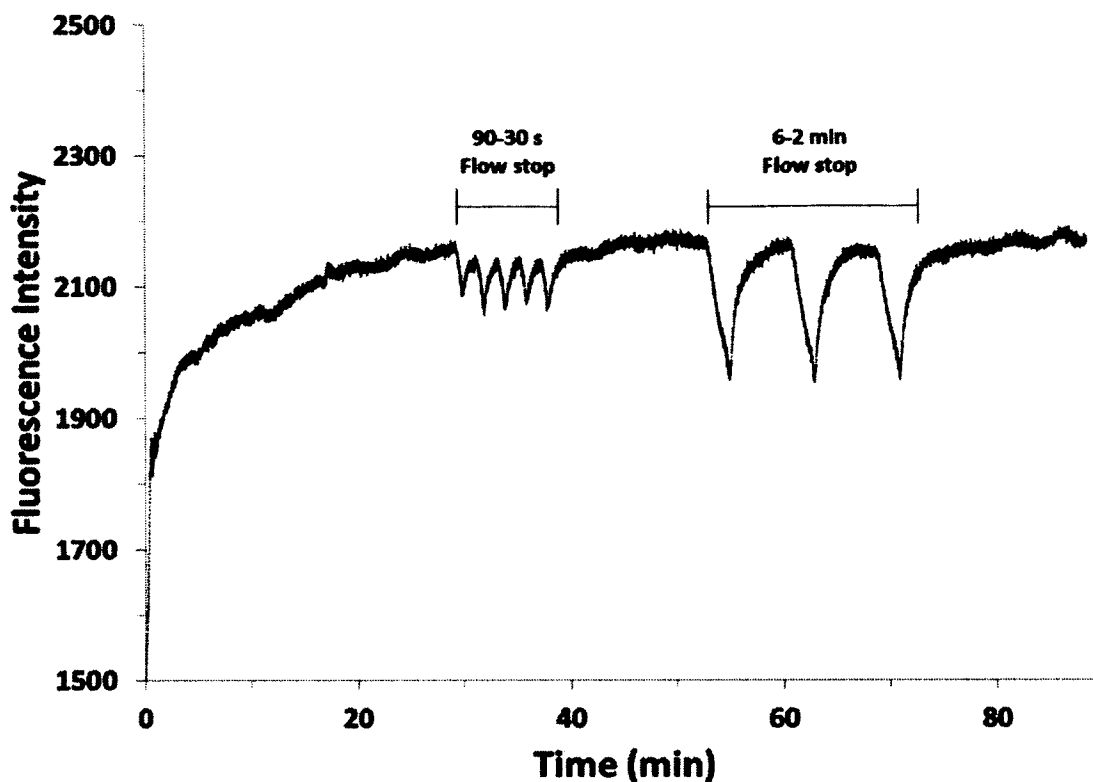


Figure 2.7. Response of PtOEP fluorescence film to 0% OW under constant flow rate and 90/30 s and 6/2 min flow/stop cycle using Prototype 2.

A commercially available oxygen sensitive fluorophore film, the RedEye[®] oxygen sensing patch from Ocean Optics (OO) with a proprietary FOXY coating (Figure 2.8), was placed in the Prototype 2 platform and under the same flow/stop cycles with 0% OW as a comparison to our PtOEP film. The OO film comprises three layers compared to two layers in the thin film developed in our lab.

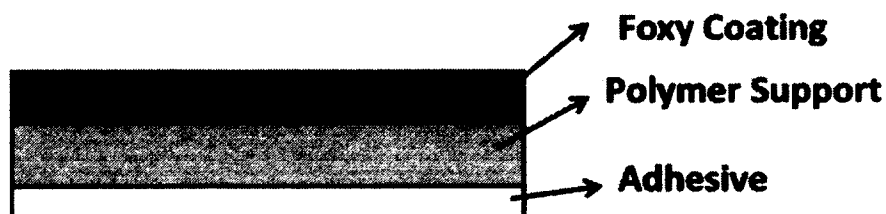


Figure 2.8. Illustration of “RedEye Oxygen Sensing Patches” from Ocean Optics.

In our film the fluorophore is embedded in the polymer layer, which helps in minimizing the thickness. The response from the OO film is shown in Figure 2.9. Although a weak response from the OO fluorophore film was observed during the 90/30 s, during the 6/2 min cycles there was no response from the sensor.

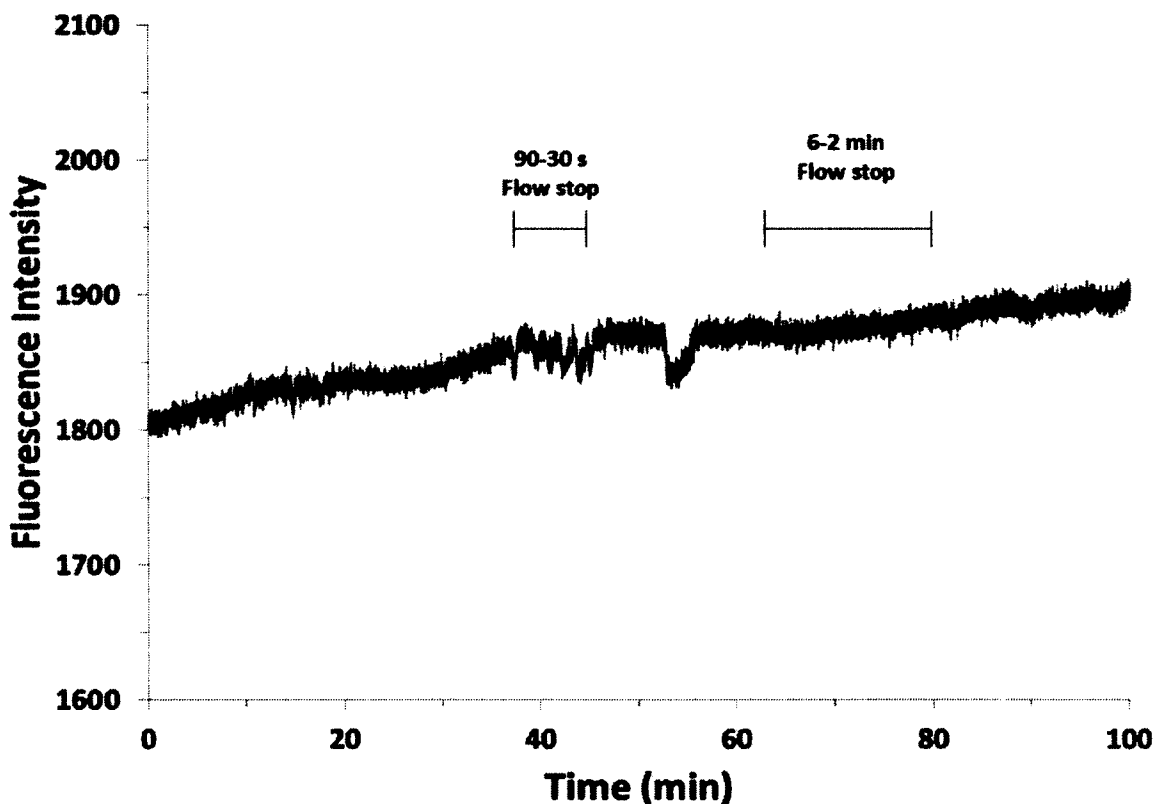


Figure 2.9. Response of commercially available Ocean Optics fluorescence oxygen sensitive “Redeye” film to 0% OW under constant flow rate and 90/30 s and 6/2 min flow/stop cycle using Prototype 2.

Finally, the data from the two Prototypes and the OO film are compared in Figure 2.10 using 0% OW under constant flow rate, using 90/30 s (A) and 6/2 min (B) flow/stop cycles. Curve 1 is the response from Prototype 1 with a fluorophore spot, curve 2 is the response from Prototype 2 with the PtOEP fluorophore film developed in our lab and curve 3 is the response from Prototype 2 with the commercial OO fluorophore film. The

PtOEP film response in Prototype 2 is superior to the thin PtOEP fluorophore film developed in our lab for Prototype I, showing slightly higher fluorescence signal sensitivity and a shorter time constant to changing oxygen concentrations. The OO film did not show a change in fluorescence intensity under different oxygen concentrations in our platform.

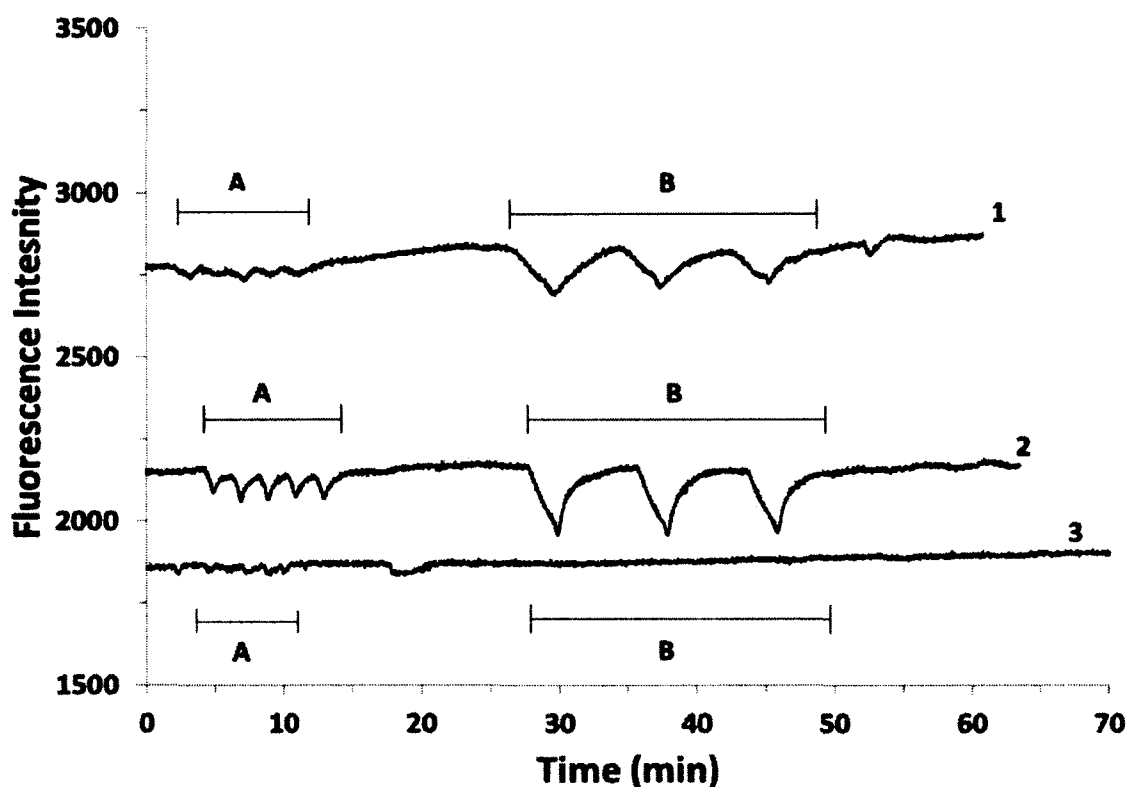


Figure 2.10. Comparison of different fluorophore film response from (1) Prototype 1 with fluorophore spot, (2) Prototype 2 with PtOEP fluorophore film, (3) Prototype 2 with Ocean Optics fluorophore film using 0% OW under constant flow rate, 90/30 s (A) and 6/2 min (B) flow/stop cycles.

2.4 Protocol for Plating *C. albicans* in a 24-Well Plate

After the design of the experimental setup was finalized, it was used to measure extracellular oxygen change in a *C. albicans* culture in a 24-well plate. Various protocols were developed to plate *C. albicans* in a 24-well plate. The first protocol was to prepare a

primary culture by picking a colony from the *C. albicans* (3153A Strain) streak plate in the refrigerator using a flamed inoculating loop. This colony was used to inoculate 5 ml of YPD media (1% yeast extract, 2% peptone, 2% dextrose in 1 L distilled water), which was incubated overnight in a 225 rpm shaker at 37°C. A 10 µl aliquot of this overnight culture of *C. albicans* was added to 2 ml of fresh YPD media in a 24-well plate. The 24-well plate was placed in an incubator at 37°C for 24 hrs so the cells could grow across the bottom of the well plate. This well plate was then used to measure the extracellular oxygen concentration changes shown in Figure 2.11.

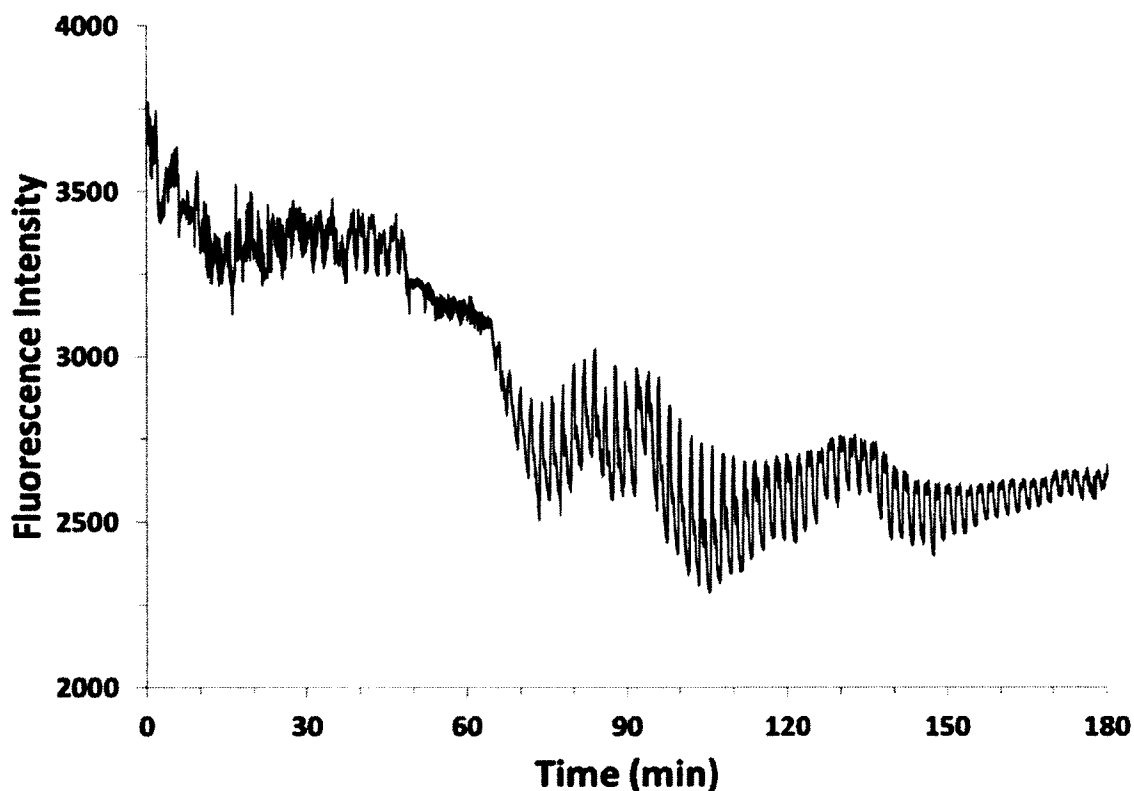


Figure 2.11. Response from *C. albicans* using Prototype 2 using first protocol using 90/30 s flow/stop cycle and 50% flow rate.

As seen in Figure 2.11 the response from *C. albicans* using the first protocol was not consistent and also difficult to understand and interpret. Although a change in the

fluorescence intensity was observed from 60 to 120 min during the stop cycle, this change slowly diminished. This response can be probably attributed to the plating protocol of *C. albicans*, where they were kept in an incubator for 24 hrs without any fresh supply of nutrients.

After understanding *C. albicans* exponential growth phase by working on different plating protocols using different concentrations the final protocol was as follows: the primary culture was prepared by picking a colony from the *C. albicans* streak plate in the refrigerator using a flamed inoculating loop. This colony was used to inoculate 5 ml of YPD media, which was incubated overnight in a 225 rpm shaker at 37°C. A 10 µl portion from this primary culture was added to 5 ml YPD media and cultured overnight in a 225 rpm shaker at 37°C. A 35 µl portion of this overnight culture was added to 5 ml of YPD media and cultured in a 225 rpm shaker at 37°C for 1 hr. A 2 ml aliquot from this culture was added to a 24-well plate (Corning® 3524) and placed on a rocker for 2 hrs in a 37°C incubator. This step allowed the cells to settle at the bottom of the well plate. The concentration of the cells was $\sim 1 \times 10^6$ per well. The data obtained using this protocol is shown in Figure 2.12.

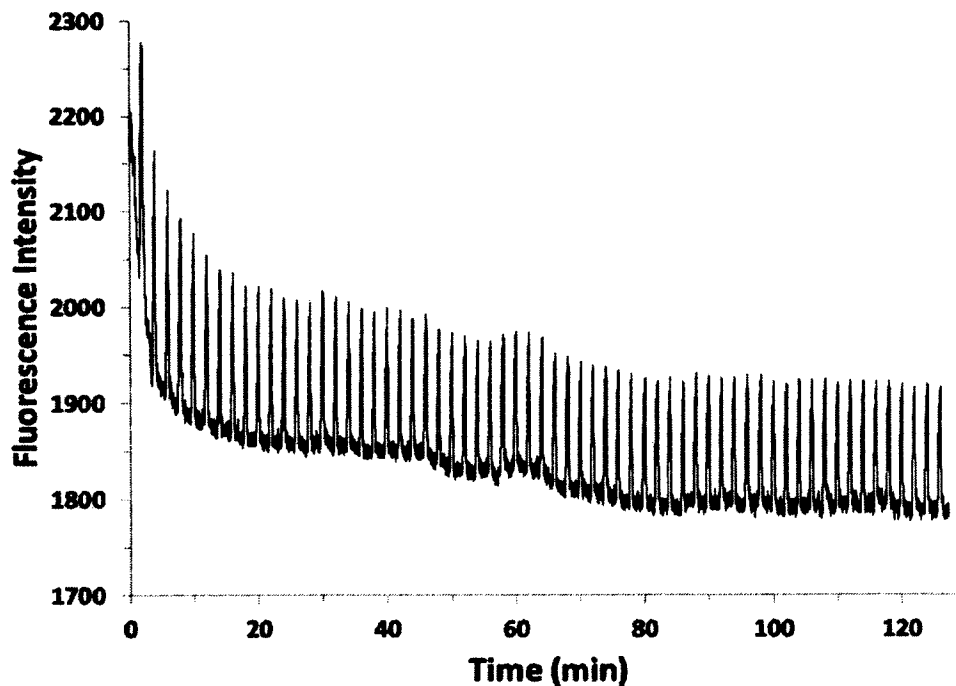


Figure 2.12. Response from *C. albicans* using Prototype 2 using final protocol using 90/30 s flow/stop cycle and 50% flow rate.

The data obtained using the final protocol showed a significant increase in the fluorescence intensity during the stop cycle, as would be expected from the consumption of oxygen by the cells. The signal returned to the baseline during flow, as oxygen was replenished to the sensor. All plating of cells followed this protocol for the experiments presented in the following chapters.

3.0 SENSOR RESPONSE TO METABOLIC ANATAGONOST AND ENHANCER

3.1 Introduction

In this chapter, a brief background of the present state of the art in metabolic measurements using fluorescent sensors will be introduced and how they relate to this study. In addition, the method of incorporation of the fluorescent oxygen sensor into the final measurement platform using the method of discontinuous transverse flow will also be presented. In order to show that the finalized sensor and measurement platform can be used to measure both decreases and increases in the extracellular oxygen consumption rates of cells, *C. albicans* was exposed to known metabolic antagonists (fluoride and 2,4-dinitrophenol) to show a decrease in oxygen consumption rates, and an enhancer (increased glucose concentrations), to show an increase in oxygen consumption rates. To ensure that the metabolites themselves were not contributing to the sensor response, the PtOEP film was tested against each antagonist and enhancer in the absence of cells, in addition to changes in temperature and ionic strength.

3.1.1 Fluorescence-Based Sensors

Presently the main approaches for performing fluorescence-based measurements with cells include the use of soluble probes, incorporation of micro/nanoparticles into the cells, thin films of analyte responsive fluorophores, and optical fiber transmission sensors [47][29]. Soluble fluorophore probes are typically added to the cell culture where they

attach to functional groups in or on the cells [48]. This attachment causes contamination of cell sample, may impair cellular function, or may have other unknown effects. The next approach uses micro/nanoparticle based sensors such as PEBBLE sensors, which are polymer or silica beads with an encapsulated fluorophore [29][49]. Although this approach can increase the photostability of the fluorophore, it can be difficult to reproduce and may exhibit particle aggregation inside the cell [47][50].

The remaining two approaches, thin film and optical fiber sensors, are of interest because they are non-invasive, as the fluorophores are embedded in an encapsulating medium located in the extracellular environment. They offer the benefits of passive sensing and non-interference with the cellular function. Thin film sensors are prepared by depositing the fluorophore on substrates such as glass or polymers using an encapsulating medium [51][52]. Fiber optic sensors may be prepared by attaching the fluorophore directly to the optical fiber, but the fluorophore coatings can lose sensitivity due to photobleaching with time and will require reapplication [53][54]. Sensors based on these processes are commercially available from Ocean Optics and PreSens, who sell thin film and fiber optics-based fluorescent sensors for research studies of cell metabolism/physiology, drug treatment, and bioenergetics [47][55][56]. Another company, Seahorse Bioscience, combined these two approaches in the XF Analyzer, an instrument that detects changes in extracellular oxygen and proton concentration for studying cell responses to drug exposure in real-time [3]. Because the measurements are performed in a static media environment, unwanted cellular metabolites build up in the media and may cause unknown stress on the cells.

3.1.2 Discontinuous Transverse Flow Platform

An illustration of oxygen flow and consumption in a transverse flow during a flow/stop cycle is shown in Figure 3.1. Our approach is to integrate the fluorescent thin film and fiber optics with the Cytosensor[®] Microphysiometer discontinuous transverse flow to overcome the limitations like cellular contamination, aggregation of particles inside the cell, and buildup of unwanted cellular metabolites. The transverse discontinuous flow (flow/stop cycle) method can provide continuous supply of fresh nutrients through media, avoid build-up of unwanted cellular metabolites, and allow the addition and removal of analytes as needed.

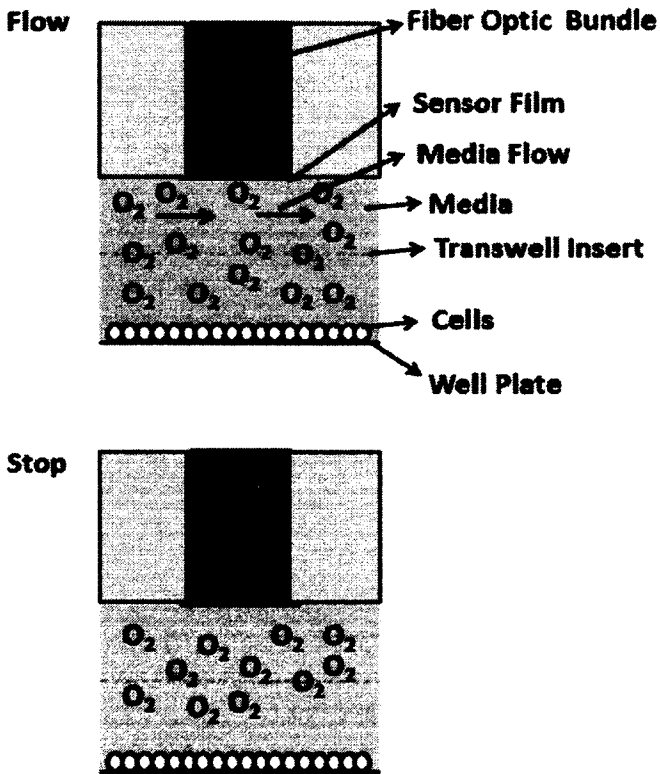


Figure 3.1. A) Oxygen during a flow cycle in transverse direction, B) Consumption of oxygen during a stop cycle. Components not to scale.

Because the transverse flow method forms a fluid barrier between the fluorescent sensor and the cells during flow cycle, we obtain a baseline sensor signal, which can be used to differentiate against the effects of other metabolites on the sensor. Another advantage of this platform is that cellular studies can be performed over a long time period if needed, from hours to days, and the sensor probe can be adapted to fit in 12-, 48- and 96-well formats. For this adaptability we developed an inexpensive (~1 cent for 1 mm disk), disposable fluorescent thin film to be used with a reusable sensor probe with an integrated fiber optic bundle that can fit in a traditional 24-well plate familiar to researchers. This measurement technique provides real-time changes in metabolite concentration, allowing researchers to interpret data during the experiment and perhaps make any modifications to the experiment protocol if needed. Real-time data can be useful to determine when cells reach a steady metabolic state, when to introduce the external metabolites, and also observe any cellular recovery after metabolite removal.

3.1.3 Platform Test Sensor: Oxygen

The metabolic analyte of interest for this measurement platform was oxygen, due to the crucial role it plays in various biological systems. The rate of cellular oxygen consumption in response to external stimuli can provide information about the cell metabolism, viability, and behavior [47][29]. A well-known oxygen sensitive fluorophore, platinum octaethylporphyrin (PtOEP), was used to develop a highly responsive thin film. PtOEP exhibits a large Stokes shift between the excitation and emission wavelengths, has a fast response time, high sensitivity, low photobleaching, and good selectivity to oxygen [57]. Fluorescence intensity was chosen to observe changes in oxygen because of its simplicity and ease of experimental setup [58]. The PtOEP film

was fixed at the end of a fiber optic bundle that was sealed in a sensor head that had been adapted to fit into a standard 24-well plate.

The utility of this fluorescent-based oxygen sensor in combination with a transverse flow/stop measurement technique is demonstrated by determination of extracellular oxygen concentration changes of *C. albicans* in response to fluoride and glucose stimulation.

3.2 Materials and Methods

3.2.1 Materials

Platinum octaethylporphyrin was purchased from Frontier Scientific, sodium fluoride (NaF, 99%) from Matheson, Coleman, and Bell, 2,4-dinitrophenol (DNP, 98%) from Eastman Organic, and dichloromethane (98%) from Acros. Yeast extract and peptone were from Becton, Dickinson and Company, and dextrose was from Sigma-Aldrich. The YPD (Yeast extract, Peptone, Dextrose) media contained 1% yeast extract, 2% peptone, and 2% dextrose. Transparent adhesive tape (Scotch 3M) was purchased locally.

3.2.2 PtOEP Film Preparation

The PtOEP fluorophore film was prepared by dissolving 0.3 mg of PtOEP in 0.5 mL of dichloromethane. A 5 μ L portion of this solution was drop cast onto the cellulose tape, making a spot approximately 3 mm in diameter, and then allowed to air dry for 24 hrs. A 2 mm diameter circular disk was cut from the film and affixed to the fiber optic bundle on the sensor head. Each PtOEP sensor disk was used for one experiment then discarded. Unused films were stored at room temperature for up to 3 months with no determinable loss in sensitivity. An image of the PtOEP film is shown in Figure 3.2.

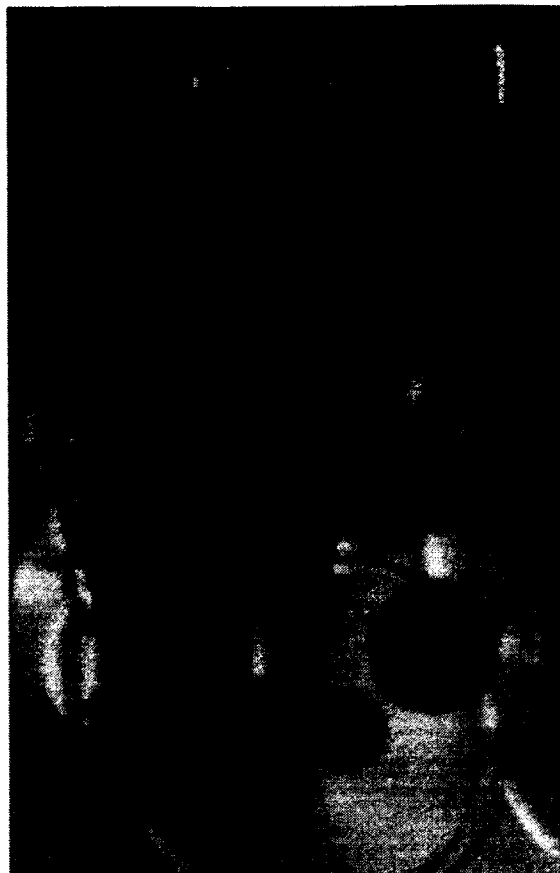


Figure 3.2. Image of various PtOEP sensor films on a cellulose tape.

3.2.3 Sensor Head Construction

A sensor head from a Cytosensor[®] Microphysiometer was modified by drilling a vertical hole through the body, then inserting an optical fiber bundle (multimode optical fiber 0.22NA, Ø365 μm from Thor labs) comprised of one excitation fiber surrounded by six emission collection fibers (Figure 3.3). The bundle was then sealed in the sensor head with epoxy (Hysol[®] epoxy-patch adhesive 0151) and polished flush with the surface.

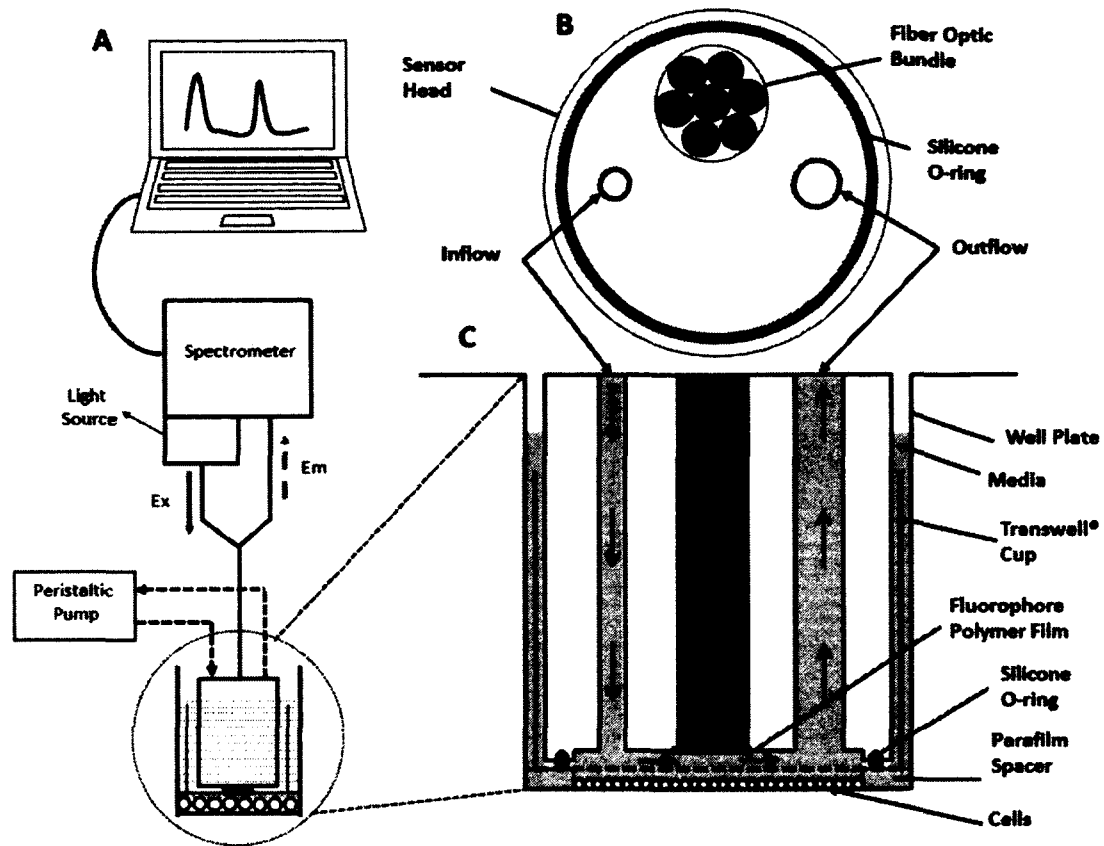


Figure 3.3. (A) Schematic of the experimental setup. (B) Face view of the modified Cytosensor[®] Microphysiometer sensor head showing the fiber optic bundle placement. (C) Cross-sectional side view of the sensor head in a well of a 24-well plate with a Transwell[®] cup.

3.2.4 Cell Culture and Plating

An aliquot of 30.0 μL from an overnight culture of *C. albicans* was inoculated into 5 mL of YPD media and incubated at 37°C in an incubator shaker at 225 rpm for 1 hr. A 2 mL portion of this cell culture was added to a single well of a 24-well plate then placed on a rocking platform in an incubator (37°C) for 2 hrs, which allowed the cells to adhere evenly across the bottom of the well. The cell count in the bottom of the well plate was approximately 1×10^6 per well.

3.2.5 Experimental Set-up and Conditions

A ring-shaped spacer (Parafilm[®] M, 127.0 μm thickness) was inserted in the bottom of the well plate with the cells, followed by a polyester membrane (3462 Corning Transwell[®], 3 μm pores). The sensor head was then inserted in the well with a slight pressure, making a seal between the o-ring, membrane, and spacer. The membrane allowed flow from the sensor head to perfuse the cells while preventing cell wash-off from shear forces during flow. The Cytosensor[®] Microphysiometer, operated with Cytosoft[®] software version 2.0.3, was used only for media perfusion and temperature control (37°C) in the well plate. A 90/30 s flow/stop cycle was used for all experiments with a flow rate of 0.15 mL/min. Fluorescence intensity measurements were obtained with an Ocean Optics USB 4000 spectrometer optimized for fluorescence and fitted with a USB-LS 395 nm excitation source. The spectrometer was controlled with Spectrasuite[®] software, which monitored and recorded the change in emission intensity with time at 646 nm every 1 s.

3.3 Results and Discussion

3.3.1 PtOEP Film Response to 0% Oxygen and Ambient Oxygen Water

As oxygen quenches PtOEP fluorescence [57], the PtOEP polymer film was initially tested in water with ambient oxygen concentration and deoxygenated water. Fluorescence intensity from the PtOEP sensor film is expected to increase when the film comes in contact with 0% oxygen water and vice versa for ambient oxygen water [36]. To test these changes, deoxygenated water and ambient water were alternately perfused across the film every 3 min. The results are shown in Figure 3.4 and indicate that the

PtOEP/cellulose film is responsive to changes in oxygen concentration and also provides reversible and reproducible data.

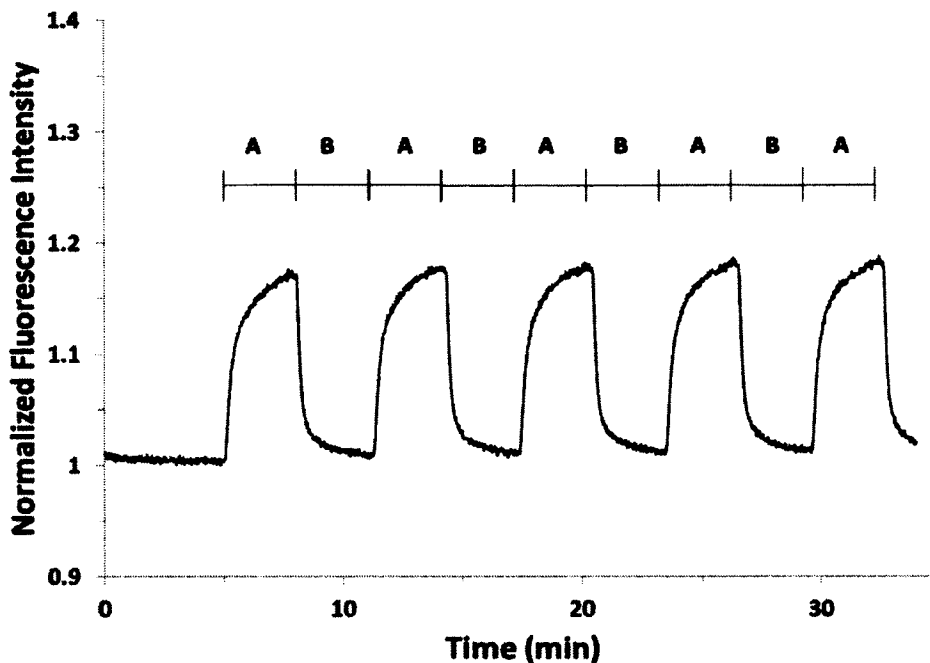


Figure 3.4. PtOEP film fluorescence response to 0% oxygen DI water (A) and ambient oxygen DI water (B). The solution is switches every 3 min.

3.3.2 PtOEP Film Response With Cells

C. albicans was plated in the well plate as described previously. As cells consume oxygen in the confined measurement space during the perfusion stop cycle, the fluorescence intensity should increase with time as the oxygen concentration decreases. When the perfusion flow cycle is resumed, the fluorescence intensity should return to the previous baseline as the oxygen concentration is replenished. This effect was confirmed by initial experiments of the PtOEP film under 90/30 s flow/stop conditions with cells. Figure 3.5 shows the intensity vs. time plot, where the increasing peaks are the intensity

measurements during the stop cycle, and the baseline is the intensity measurements during the flow cycle.

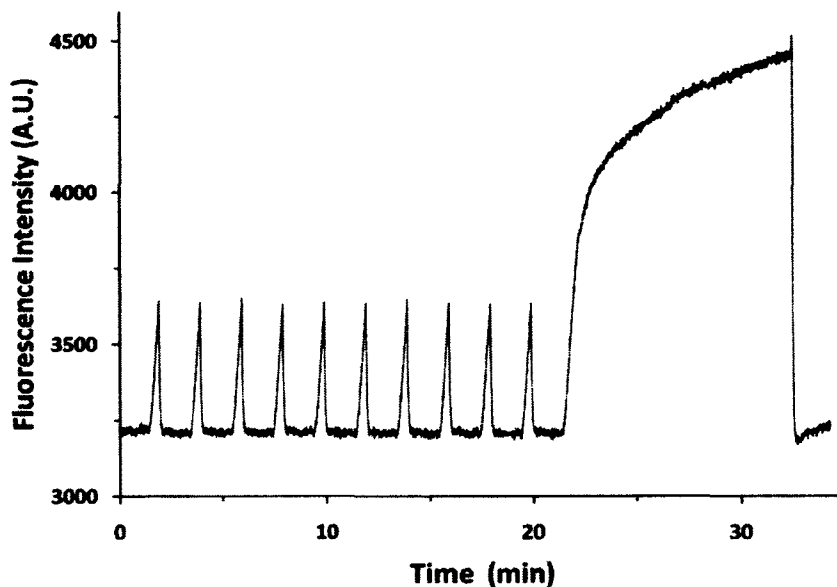


Figure 3.5. PtOEP film fluorescence response to *C. albicans* oxygen consumption during YPD media perfusion using a 90/30 s flow/stop cycle. A longer stop cycle can be seen after 21 min.

Although the peaks appear to increase linearly during the regular 30 s stop cycles, at longer stop cycles the fluorescence intensity is expected to taper off and eventually reach a steady state as the oxygen in the measurement chamber is depleted. This hypothesis was confirmed by the longer stop cycle seen in the Figure 3.5 beginning after 21 min, where the apparent linear increase in fluorescence begins to taper off toward a steady state after about 1 minute.

3.3.3 PtOEP Film Response During Different Flow/Stop Cycles With Cells

Although a 90/30 s flow/stop cycle has been a typical cycle used in the literature from other Cytosensor[®] Microphysiometer experiments, an experiment was performed to determine the flexibility of the flow/stop cycle for this platform, and whether the 90/30 s

cycle could be used so that data could be compared across platforms. The results of flow/stop cycle times at 45/15, 40/20, 90/30, 75/45, 60/60, 90/90 s can be seen in Figure 3.6. An optimal flow/stop cycle will have a maximum possible signal change during the stop cycle and a long enough flow cycle to allow analyte perfusion and washout any cellular waste products. A longer stop cycle (60, 90 s) could result in a disproportionate stress on the cellular metabolism due to the limited availability of oxygen in their confined measurement area and cause the fluorescence intensity to deviate from linearity, as seen in Figure 3.6. The 90/30 s flow/stop cycle also allows our data to be compared with the previous Microphysiometer.

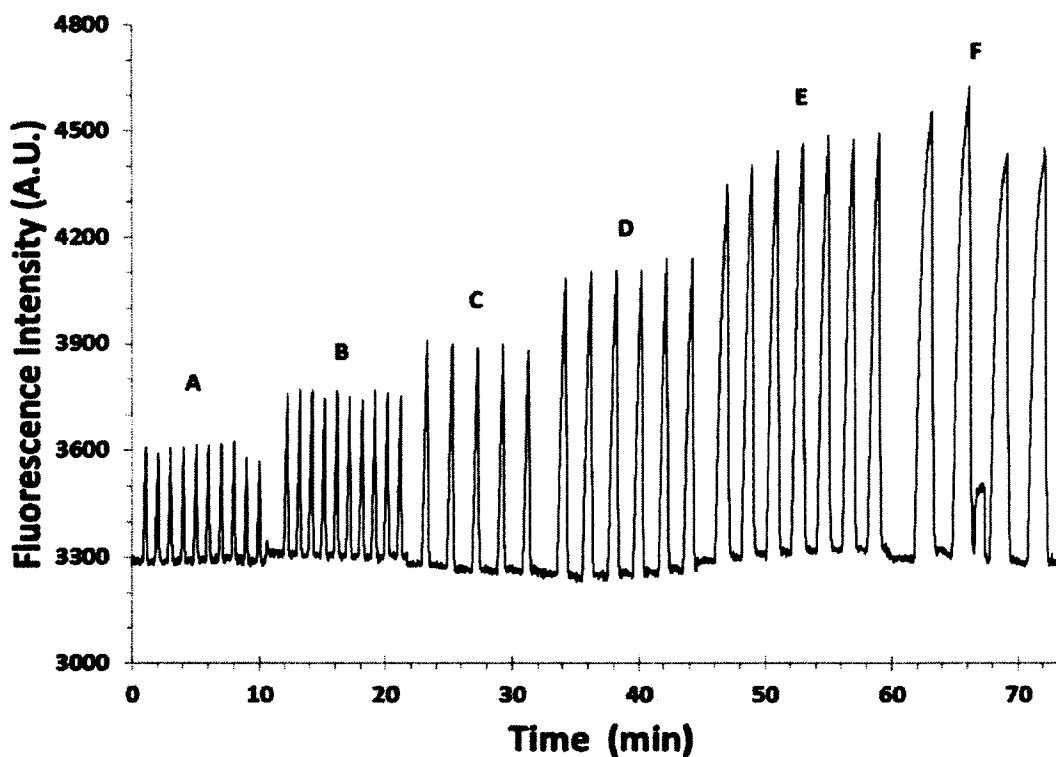


Figure 3.6. Response of PtOEP/cellulose film with *C. albicans* to varying flow/stop cycles (A) 45/15, (B) 40/20, (C) 90/30, (D) 75/45, (E) 60/60, (F) 90/90 s.

3.3.4 PtOEP Film Response With No Cells

With no cells present in the measurement chamber, the fluorescence intensity was expected to remain at the baseline during both flow and stop cycles, since the oxygen concentration should not change with time. However, initial experiments without the cells revealed a slight decrease in the intensity during the stop cycle. To determine if this decrease was caused by changes in temperature from the incoming media during the start of the flow cycle, an experiment was performed (Figure 3.7, Curve 2) in which the sensor was first allowed to equilibrate in room temperature water (23.4°C), followed by perfusion with cold water (5.7°C) from 70 to 92 minutes (Figure 3.7, bracket A), then warm water (53.6 °C) from 116 to 138 minutes (Figure 3.7, bracket B). As seen in Figure 3.7, there were no significant changes in the fluorescence intensity from different water temperatures during either the flow or stop cycles. Curve 1 has been included as a comparison of the sensor response with cells (no temperature changes).

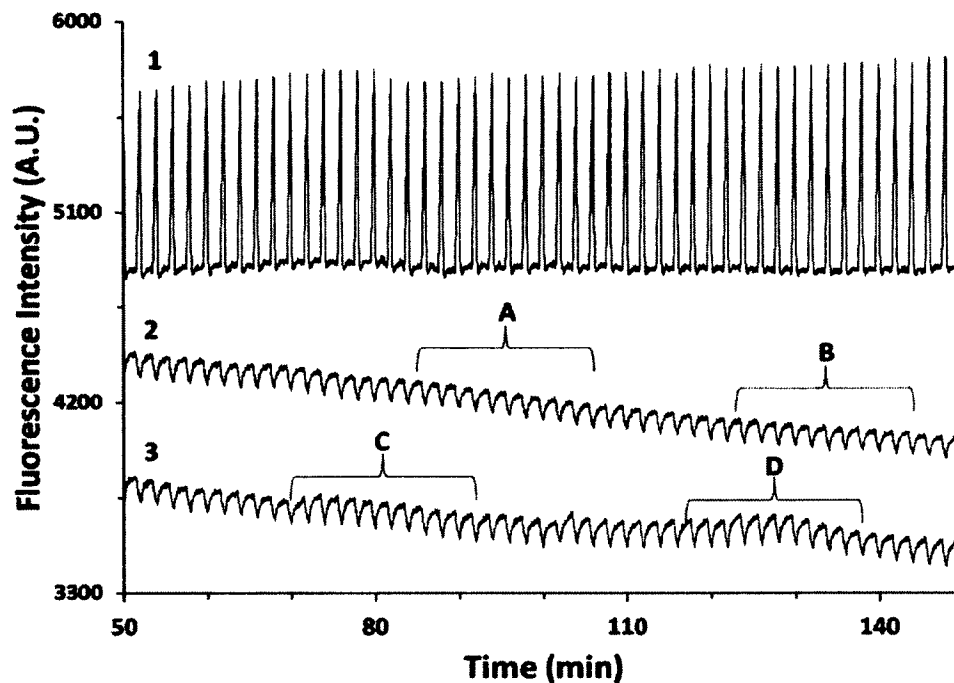


Figure 3.7. Changes in PtOEP film fluorescence intensities (untreated data) with 90/30 s flow/stop cycles in response to 1) *C. albicans* with YPD media perfusion, 2) no cells with changing water temperature (initial = room temp, A = cool, B = warm), and 3) no cells with YPD media perfusion followed by YPD/NaF (C) and DI water (D).

The PtOEP film was also tested against negative controls that would be encountered in the measurement environment. Since NaF would be added to the cells as an antagonist, the film was subjected to YPD media with and without 50 mM NaF when no cells were present. The addition of YPD and NaF is shown in bracket C of Figure 3.7, where a slight increase in the baseline can be seen with the introduction of NaF, although the change is not significant in comparison to the intensity changes when cells are present. Since glucose would be added as a metabolic enhancer, bracket D of Figure 3.7 shows the effect of replacing the YPD media (which contains glucose, growth factors, and various ions) with pure water. The slight baseline shift in the fluorescence intensity also appears to be insignificant in comparison to intensity changes from the cells. Although the fluorescence baseline drift observed in Figure 3.7 is likely due to the known

photodegradation properties of PtOEP [41][59][60], this effect has been minimized by the conversion of raw fluorescence data to normalized peak height discussed later.

3.3.5 Response of Sensor to Changing Oxygen Consumption Rates

To demonstrate the utility of the PtOEP sensor in determining changes in oxygen consumption rates from cells stimulated by various analytes, antagonists (NaF, DNP) were used to decrease the oxygen consumption rates, and an enhancer (glucose) was used to increase the oxygen consumption rates.

NaF is a known inhibitor of enolase enzyme during the glycolysis cycle [61]. Inhibition of glycolysis stops the metabolic growth of *C. albicans*, causing them to enter a dormant state [62]. When cells are in a dormant state, the rate of oxygen consumption should diminish, which should be indicated by a decrease in fluorescence intensity of the sensor during the stop cycles.

The cells were plated into a 24-well plate as described previously and placed in the measurement apparatus. After equilibration in YPD media under the 90/30 s flow/stop cycles to establish a baseline metabolic rate (Figure 3.8), the cells were exposed to 50.0 mM NaF for first 20 minutes (from 128 to 148 minutes), then after a period of recovery for 16 minutes (from 190 to 206 minutes). In both cases a decrease in stop cycle fluorescence intensity can be seen during the NaF exposure. This decrease was in agreement with our hypothesis that the fluorescence intensity should decrease upon cell exposure to NaF in the perfusion media. When NaF perfusion was discontinued the fluorescent intensity peaks during the stop cycles increased back to previous levels, indicating a recovery of cell metabolic activity. It can also be seen in Figure 3.6 that the rate of decreasing oxygen consumption is smaller during the second NaF exposure than

during the first NaF exposure. Subsequent experiments confirmed this observation. One possibility for this difference could be *C. albicans* during the first NaF exposure might explore other metabolic pathways to sustain their metabolism and use those pathways during the second NaF exposure [63][64]. Although the chemical pathways involved for this resistance has not been studied yet, it has been reported previously by Hongslo et al., that mouse fibroblasts cultured in the presence of 6mM NaF have sustained resistance to 6mM or lower concentration of NaF even after two years (~700 generations) [65].

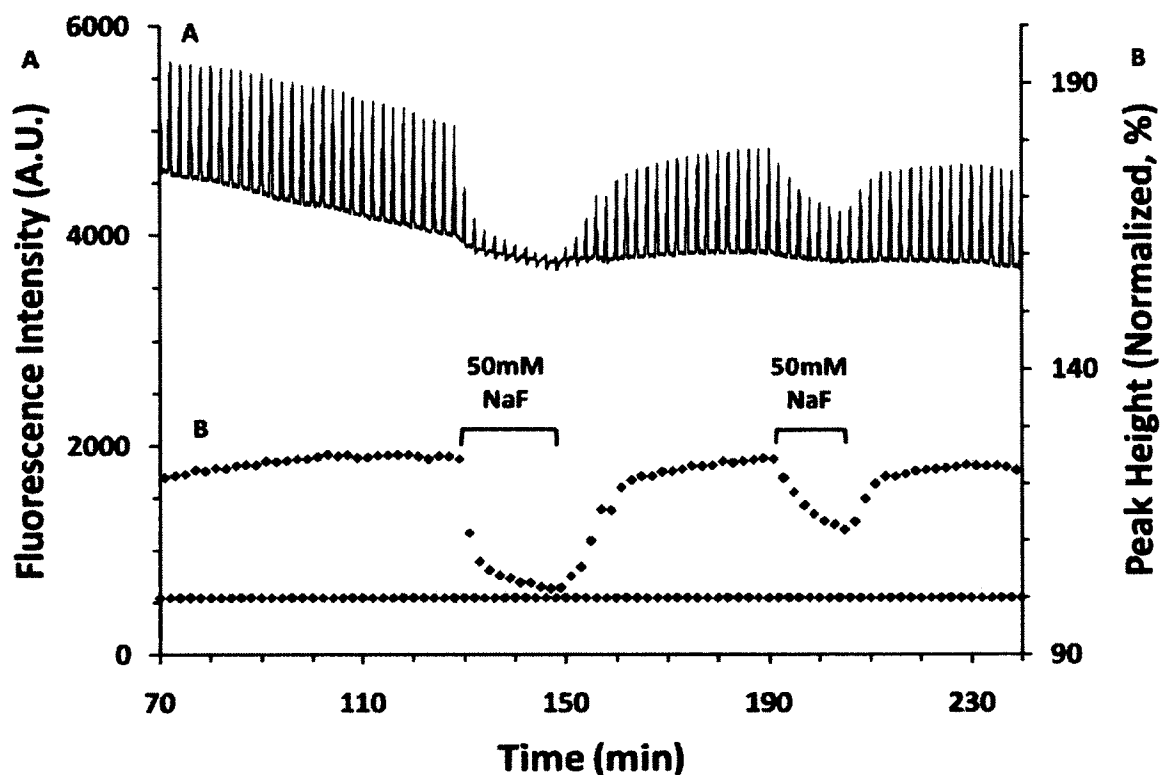


Figure 3.8. A) Raw fluorescence intensity data of *C. albicans* upon treatment with 50 mM NaF. B) Raw data peak heights normalized to baseline (100%). Each data point above 100% represents one 90/30 s flow/stop cycle.

3.3.6 Conversion of Raw Data to Normalized Peak Height

During the stop cycle, the cells consume oxygen in the confined volume under the sensor head, thus depleting the oxygen concentration at the sensor. PtOEP fluorescence has an inverse relationship with oxygen concentration, thus fluorescence intensity is expected to increase as O₂ levels decrease. During the flow cycle, the PtOEP sensor measures the relative oxygen concentration of the YPD media alone, providing a baseline against which to measure changing oxygen consumption rates during the stop flow. Thus, the peak fluorescence intensity during each stop cycle was normalized to its previous flow cycle fluorescence intensity baseline, according to the following equation:

$$I_N = \left(\frac{I_{\max}}{I_0} \right) \times 100 \quad \text{Equation 3.1}$$

where I_N is the normalized fluorescence intensity of each stop/flow cycle, I_{\max} the maximum fluorescence intensity during the stop cycle, and I_0 the average fluorescence intensity of the baseline during the previous flow cycle. This normalization helped correct for any fluorescence baseline drift and intensity changes of the sensor itself, and provided better visualization of the effect of analytes on cell metabolism (Figure 3.8).

3.3.7 Response of Sensor to Different Concentrations of NaF

Next, different concentrations of NaF were used to explore the possibility of establishing a dose-response relationship. The cells were plated in a 24-well plate as described previously and a 90/30 s flow/stop cycle was used. Varying concentrations of NaF (5, 10, 25, and 50mM) were perfused during the stop cycles for 10 min each from 126 to 166 min. No significant change in the peak height was observed from 126 to 166 min as seen in Figure 3.9. After discontinuing NaF perfusion the metabolic activity of

the cells increased and reached a steady state. When the cells were exposed to a higher concentration (100mM) of NaF from 262 to 284 min, the cellular metabolism decreased, which can be seen as smaller peak height in Figure 3.9.

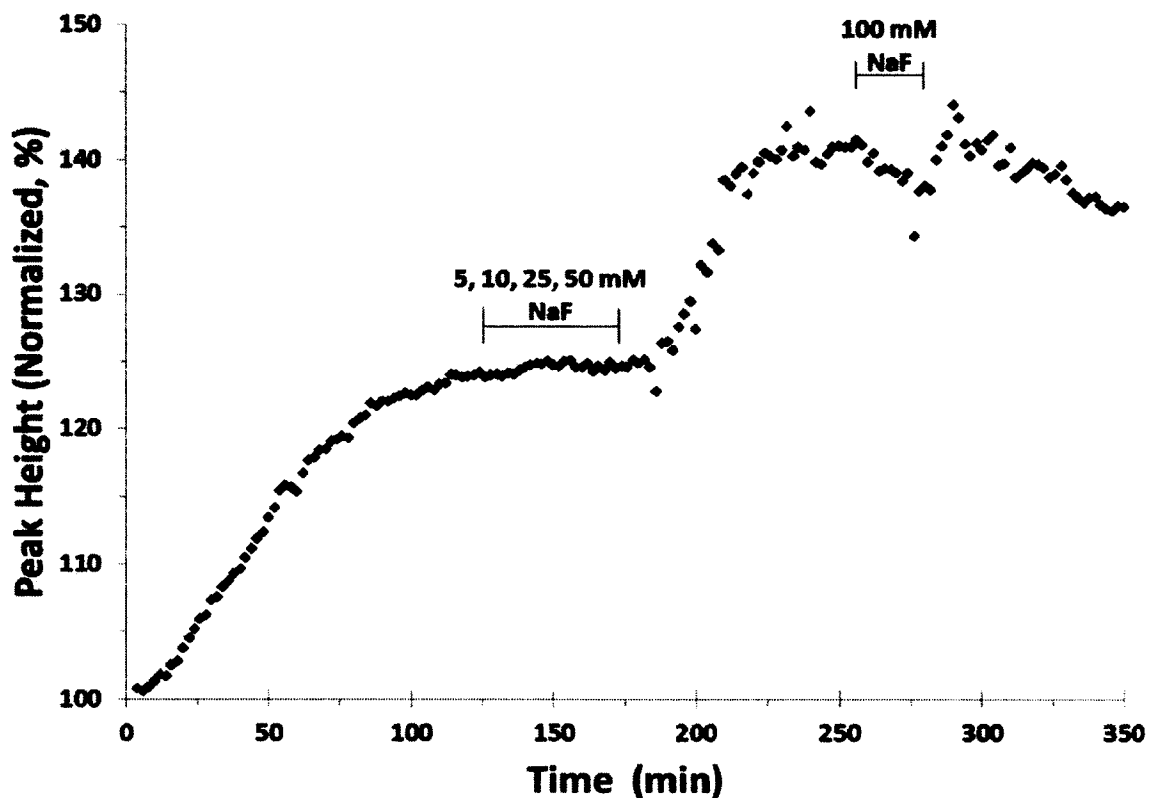


Figure 3.9. Effect of different concentration of NaF 5mM (126 to 136 min), 10mM (136 to 146 min), 25mM (146 to 156 min), 50mM (156 to 166 min), 100mM (262 to 284 min) on the oxygen consumption rates of *C. albicans*.

When the cells were exposed to increasing concentrations of NaF the fluorescence intensity remained constant, which could be the cells getting acclimatized to low concentrations of NaF and exploring other cellular pathways to maintain their metabolism [63]. After the removal of NaF perfusion, oxygen consumption increased and reached a steady state. When 100mM NaF was introduced, its effect on the cellular

metabolism was also minimal; one possibility being that the cells used other available cellular pathways to sustain their metabolic activity.

3.3.8 Response of Sensor to DNP

DNP was the second metabolic antagonist used, which is known to uncouple oxidative phosphorylation in mitochondria at concentrations greater than 50 μM [66]. A modified Cytosensor[®] Microphysiometer was used to study the effect of 0.5 mM DNP on oxygen consumption rates of Chinese hamster ovary (CHO) cells [2] using electrochemical sensors as seen in Figure 3.10. The rate of oxygen consumption decreased under the effect of DNP and returned back to the baseline after it was removed.

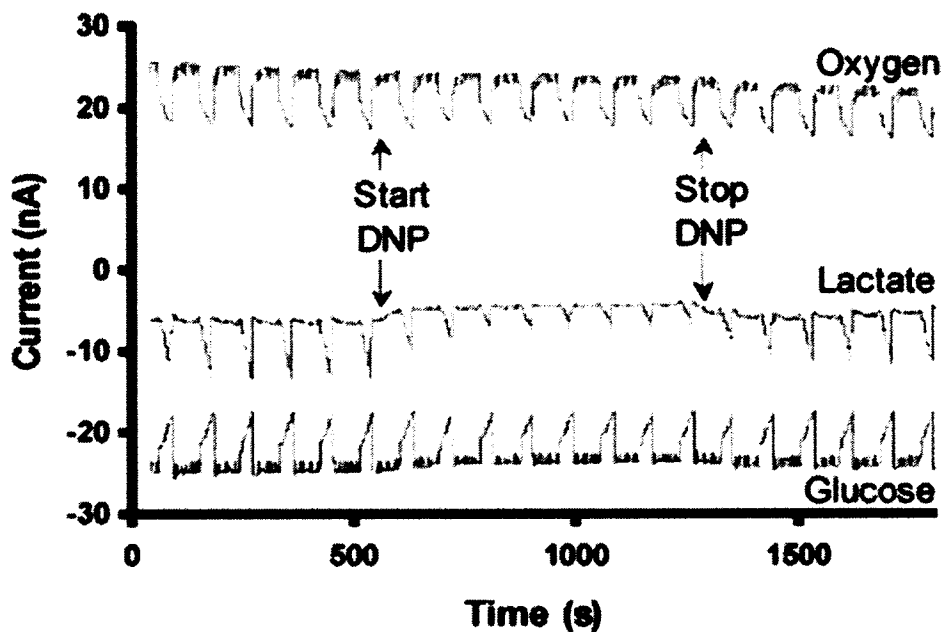


Figure 3.10. Raw data for glucose, lactate, and oxygen response to the addition of 0.5 mM DNP to CHO cells in the modified Microphysiometer. The pump cycle consisted of a 60-s flow and 30-s stop-flow phase [2].

To test the effect of 4 mM DNP on *C. albicans*, cells were plated in a 24-well plate as described previously. A 90/30 s flow/stop cycle was used so the cells could attain a basal metabolic rate. The cells were exposed to 4 mM DNP for 22 min (from 222 to

244 min) where a decrease in the peak height can be seen in Figure 3.11, which is in agreement with Eklund et al. [12].

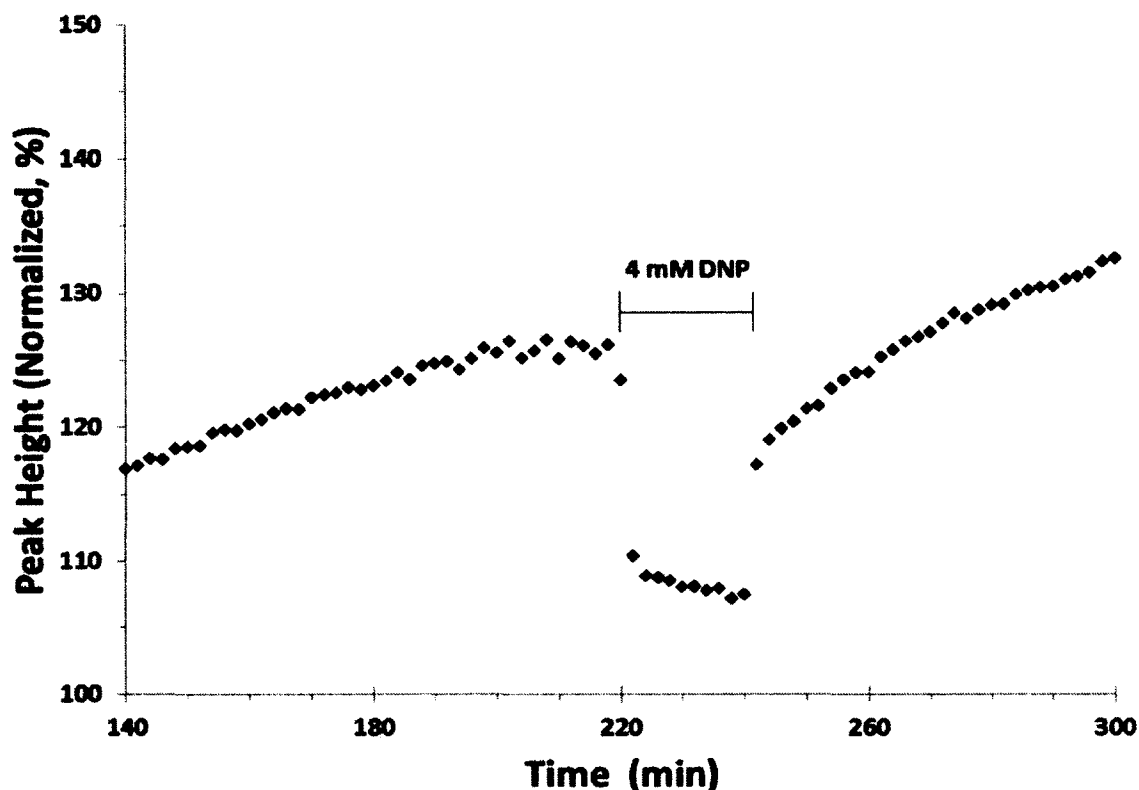


Figure 3.11. Effect of 4mM DNP (222 to 244 min) on the oxygen consumption of *C. albicans*. The decrease in the oxygen consumption of cells can be observed in the presence of DNP.

3.3.9 *C. albicans* Response to Glucose Stimulation

To show that this measurement technique is also responsive to increases in oxygen consumption rates, *C. albicans* cells were first conditioned to grow in YPD media with 0.5% glucose, then exposed to YPD media with 2.0% glucose. Upon exposure to an increased energy source, the oxygen consumption of the cells should increase as a result of increased metabolism [66]. This increase can be seen in Figure 3.12 where, following the growth phase, *C. albicans* cells reached a steady state oxygen consumption rate

between 60 and 150 minutes under 0.5% glucose YPD media. Upon perfusion with 2.0% glucose YPD media, the cell oxygen consumption rate increased by nearly 50%.

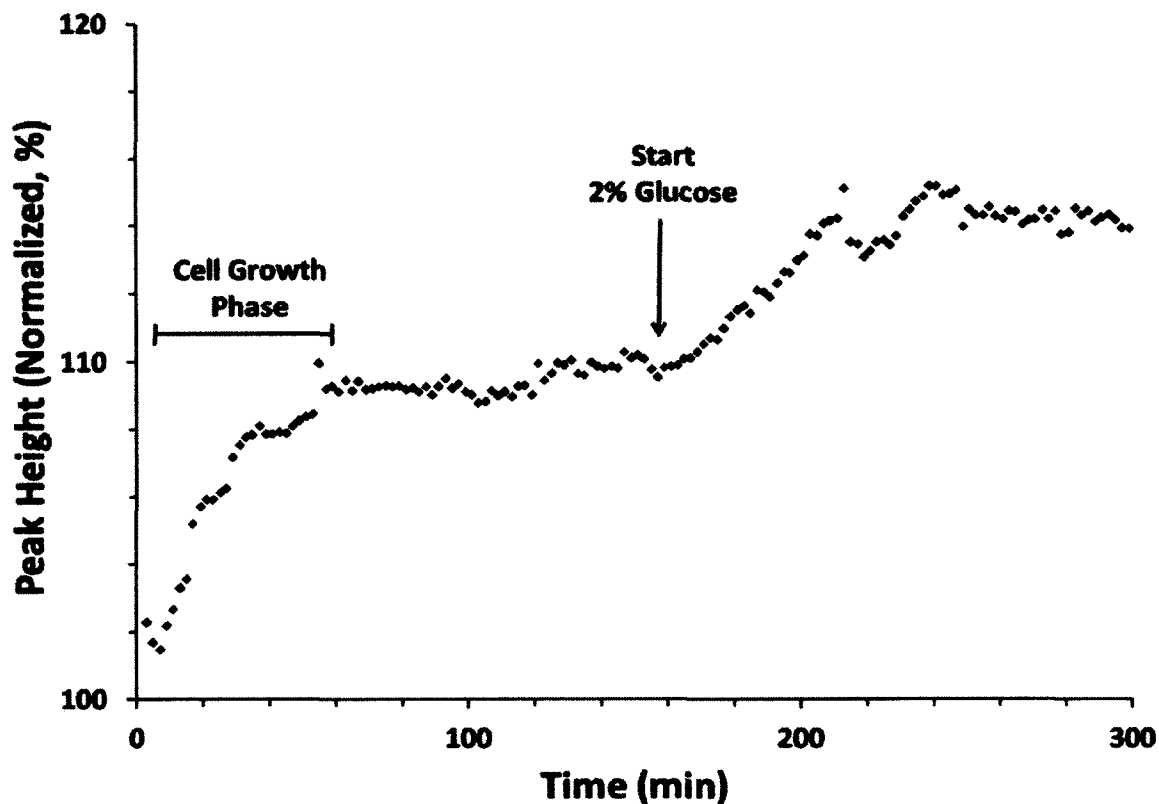


Figure 3.12. Effect of increasing glucose concentrations (0.5% to 2%) on the oxygen consumption rate of *C. albicans*. Upon addition of YPD with 2% glucose, the rate of increasing fluorescence intensity increases by nearly 50%, indicating an increase in the oxygen consumption rate of the cells by nearly 50%.

3.4 Conclusions

The utility of the fluorescence-based sensor in a transverse flow/stop measurement platform was demonstrated from real-time changes in oxygen consumption rates from *C. albicans*. The sensor can be used in standard 24-well plates common to research labs, has facile preparation, and is robust against changing media conditions. During stop cycle time intervals less than 1 minute the sensor exhibits a fast, positive

linear slope to decreasing oxygen concentrations in the measurement chamber. Baseline correction of the peak is useful for offsetting any fluorescence drift or degradation.

4.0 C. ALBICANS RESPONSE TO ANTIFUNGALS

4.1 Introduction

As reported in the previous chapter a new real-time measurement platform using an oxygen sensor that can fit in a 24-well plate was developed. This fluorescent sensor was previously used to detect increases and decreases in extracellular oxygen consumption rates of *C. albicans* when exposed to fluoride and glucose respectively. In this chapter this fluorescent sensor will be used to study the effect of antifungal drugs on *C. albicans*.

C. albicans, an opportunistic fungal pathogen, is the fourth most common hospital-acquired infection in the U.S. and is responsible for billions of dollars spent annually for its treatment [67]. Patients undergoing treatments such as organ transplants, chemotherapy, and HIV infection management are highly susceptible to these opportunistic pathogens because of their immune-compromised conditions [68]. Present treatment therapies rely on antifungal drugs, but since humans and *C. albicans* are eukaryotic and share many biological processes [67][69][70][71], these drugs also cause damage to organs in the human body.

Four classes of antifungal drugs are used to treat *C. albicans* infections: azoles, echinocandins, polyenes, and allylamines. All four classes exhibit antifungal activities by either inhibiting the ergosterol pathway, direct interaction with ergosterol in the

membrane, or disrupting the cell wall. Ergosterol is an important constituent of the fungal cell membrane and is structurally similar to cholesterol in humans.

The polyene Amphotericin B is the most effective antifungal drug, and is usually the first drug of choice in treating *C. albicans* infections. The antimicrobial activity of Amphotericin B is in binding to ergosterol, where it forms pores that disrupt the cell membrane, allowing leakage of ions into and out of the cell. Amphotericin B also binds to cholesterol in eukaryotic cells, which accounts for its high toxicity in humans [71][72][73].

More recently developed drugs, like azoles and allylamines, exhibit fewer side effects in humans and are becoming more commonly used as antifungals to treat *C. albicans* infections. Azoles inhibit the enzyme ERG11, a fungal cytochrome P450 enzyme 14 α -demethylase, which plays a key part in the ergosterol pathway. *C. albicans* responds by either inducing mutations at the binding site of ERG11 or by decreasing the ERG11 gene product minimizing the amount of target or by increasing ERG11 thereby diluting the azole. By targeting ERG11 azoles deplete ergosterol, which causes accumulation of toxic ergosterol precursors such as lanosterol, 4,14-dimethylzymosterol, and 24-methylenedihydrolanosterol, resulting in decreased membrane fluidity and fungal toxicity [74][75][76].

The effects of these and other antifungals on *C. albicans* metabolism is still not fully understood, and *C. albicans* has been shown to respond in varied and complex ways to different stresses. Measuring the change in rate of extracellular analyte production or consumption when *C. albicans* is exposed to antifungals can help researchers in understanding the pathways and enzymes involved and in designing new antifungal

drugs. One analyte that is of interest is enolase enzyme. Enolase helps *C. albicans* bind to the gastrointestinal (GI) tract in humans by interacting with extracellular matrix proteins like fibronectin and laminin [77][78][79]. The GI tract is one of the main reservoirs for *C. albicans* in immunocompromised patients, and it facilitates spread to other organs in the human body by translocation [80]. Patients for whom enolase is found in the culture medium and blood sample are determined to have invasive candidiasis. Research is in progress to understand the role enolase plays in *C. albicans* pathogenesis [78][81][82]. In this chapter we would like to understand how *C. albicans* treated with antifungals respond to sodium fluoride, a known inhibitor of enolase enzyme.

In order to test the efficacy of newly conceptualized antifungal therapies and any synergistic effects, researchers use *in vitro* studies such as optical density measurements. An *in vitro* technique that can measure the effect of the antifungals in real-time and with flexibility to introduce the antifungals either concurrently or consecutively would aid researchers in studying the effect of antifungals on the metabolism of *C. albicans*. Data obtained in real time can be useful for interpreting the effects of antifungals on *C. albicans* and help researchers to make modifications during the experiment (i.e. adding higher/lower concentration of antifungal). Experiments that use this type of modification could provide better understanding than what the experiment was initially planned for. Our hypothesis is that exposure of *C. albicans* to inhibitory concentrations of antifungals leads to cellular degradation and death, which in turn changes the oxygen consumption rates of the cells. The change in oxygen consumption can be detected by our oxygen sensor and platform described in the Chapter 3.

4.2 Materials and Methods

4.2.1 Materials

Yeast extract and peptone were from Becton, Dickinson and Company, dextrose was from Sigma-Aldrich. Amphotericin B, fluconazole and miconazole were from VWR. Platinum octaethylporphyrin (PtOEP) was from Frontier Scientific, sodium fluoride (NaF) from Matheson Coleman and Bell, and dichloromethane (CH₂Cl₂) from Acros.

4.2.2 Cell Culture

Yeast extract, Peptone and Dextrose media (YPD) consisted of 1% yeast extract, 2% peptone, 2% dextrose in 1 L distilled water. Primary culture was prepared by selecting a colony from a *C. albicans* (3153A Strain) streak plate, refrigerated at 4 °C using a flamed inoculating loop. This colony was used to inoculate 5 ml of YPD media, which was incubated overnight in a 225 rpm shaking incubator at 37°C. A 10 µl portion from this primary culture was added to 5 ml YPD media and cultured overnight in a 225 rpm shaking incubator at 37°C. A 35 µl portion of this secondary culture was added to 5 ml of YPD media and cultured in a 225 rpm shaking incubator at 37°C for 1 hr. A 2 ml aliquot from this culture was added to a 24-well plate (Corning® 3524) and placed on a rocker for 2 hrs in a 37°C incubator. This step allowed the cells to settle at the bottom of the well plate. The concentration of the cells was $\sim 1 \times 10^6$ per well.

4.3 Results and Discussion

4.3.1 Correlation Between PtOEP Polymer Film, Oxygen, and Cells

Oxygen is a known quencher of PtOEP fluorescence [57], so the fluorescence intensity from the PtOEP/polymer film and the extracellular oxygen concentration have an inversely proportional relation. During the 90 s flow cycle, media is perfused across

the film and a constant fluorescent intensity is observed as the sensor measures the oxygen concentration of the media. When the flow is stopped for 30 s, metabolically active cells consume oxygen in the confined volume under the sensor, which can be observed as an increase in fluorescence intensity. When the 90 s flow cycle is resumed the fluorescence intensity decreases and returns to the previous baseline due to replenishment of oxygen by the media. The hypothesis is when *C. albicans* comes in contact with a metabolic antagonist/enhancer or antifungal their metabolic function is affected, which leads to a decrease/increase in oxygen consumption and it can be observed in real-time using the measurement technique.

4.3.2 *C. albicans* Response to NaF

A metabolic antagonist (NaF) was used to demonstrate the relationship between cell metabolism, oxygen and peak height. NaF affects cell metabolism by inhibiting the function of enolase, an enzyme required during the glycolysis cycle [83][62]. The hypothesis is when *C. albicans* comes in contact with NaF their metabolism and resulting oxygen consumption decreases and causes the fluorescence intensity to change. *C. albicans* was plated in a 24-well plate as described previously and placed on the Cytosensor[®] platform and YPD media was perfused for 188 min. *C. albicans* was then exposed to 50 mM NaF from 188 to 210 min and again from 290 to 312 min as seen in Figure 4.1.

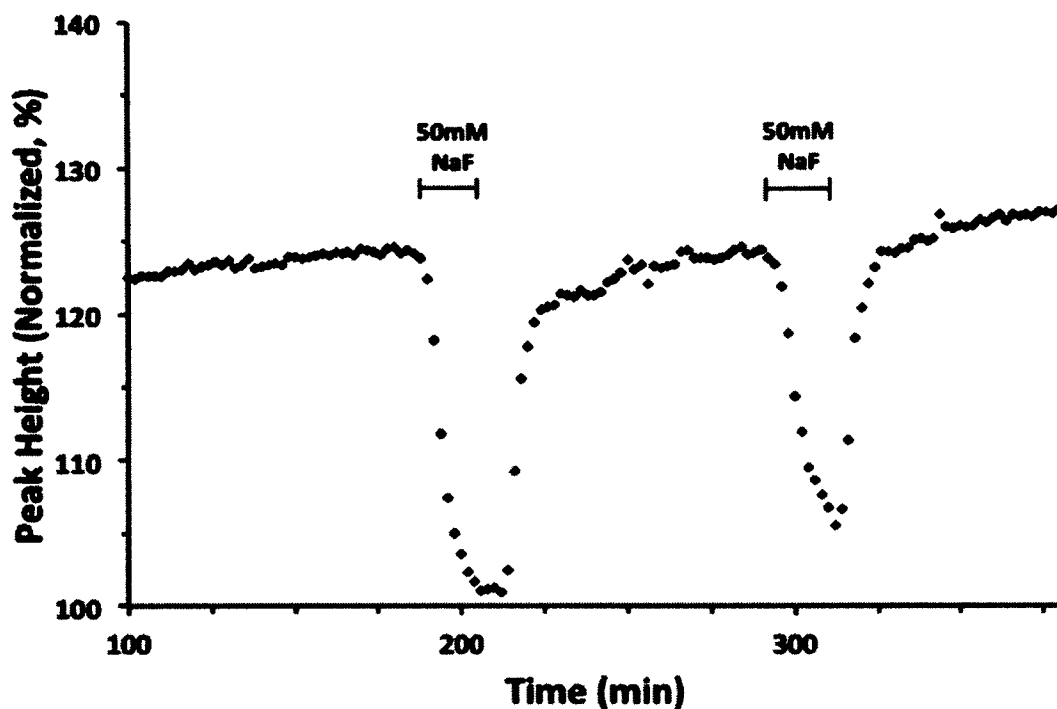


Figure 4.1. *C. albicans* response to 50mM NaF from 188 to 210 min and 290 to 312 min using 90/30 s flow/stop cycle and 50% flow rate.

Figure 4.1 shows that the cellular oxygen consumption of *C. albicans* decreased upon introduction of NaF. When NaF perfusion was discontinued the cellular metabolism recovered and reached its previous baseline, which indicates the recovery of cellular metabolic activity. This result supports our hypothesis and demonstrates that the relation between peak height, cell metabolism, and extracellular oxygen concentration can be understood for this measurement technique.

4.3.3 *C. albicans* Response to Amphotericin B

The measurement technique was next used to measure the response of *C. albicans* to amphotericin B (AMB), a known fungicide. The hypothesis being *C. albicans* extracellular oxygen consumption should decrease when exposed to AMB and it should be detected as a change in peak height by our technique. *C. albicans* was plated in a 24-well plate, as described previously, and placed in the Cytosensor[®] platform. After the

cellular metabolism reached a steady state, 2 $\mu\text{g}/\text{ml}$ AmB was introduced from 46 to 188 min as seen in Figure 4.2.

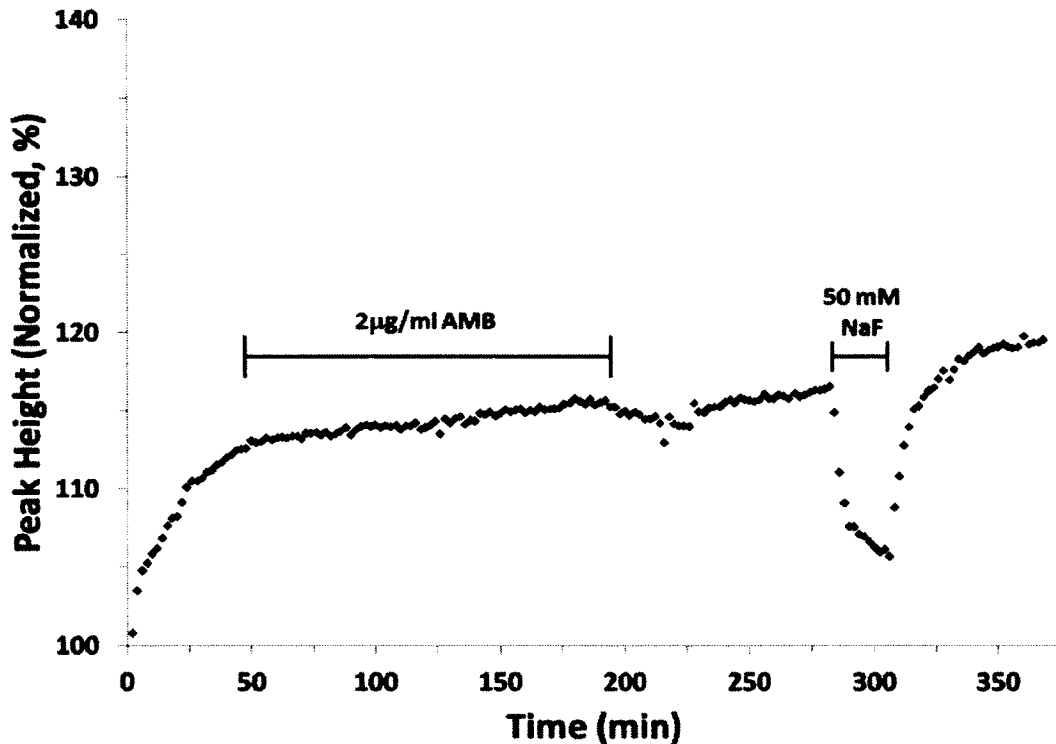


Figure 4.2. *C. albicans* response to 2 $\mu\text{g}/\text{ml}$ AMB (46 to 188 min) and 50mM NaF (338 to 360 min) using 90/30 s flow/stop cycle and 50% flow rate.

The extracellular oxygen consumption rate of *C. albicans* did not decrease after the introduction of AMB. It maintained a steady state, even after the AMB perfusion was discontinued. This lack of change may be because the AMB concentration was not effective enough to cause cell death. Next, 50mM NaF, a known metabolic antagonist, was perfused across from 282 to 304 min to determine if it would have the same effect as observed previously. The peak height decreased as expected and recovered after the 50 mM NaF perfusion was stopped.

The measurement platform was next used to observe the effect of a higher concentration of AMB (4 $\mu\text{g/ml}$) using the same conditions and parameters for 2 $\mu\text{g/ml}$ AMB. After the cellular metabolism reached a steady state, 4 $\mu\text{g/ml}$ AMB was perfused from 50 to 282 min (Figure 4.3).

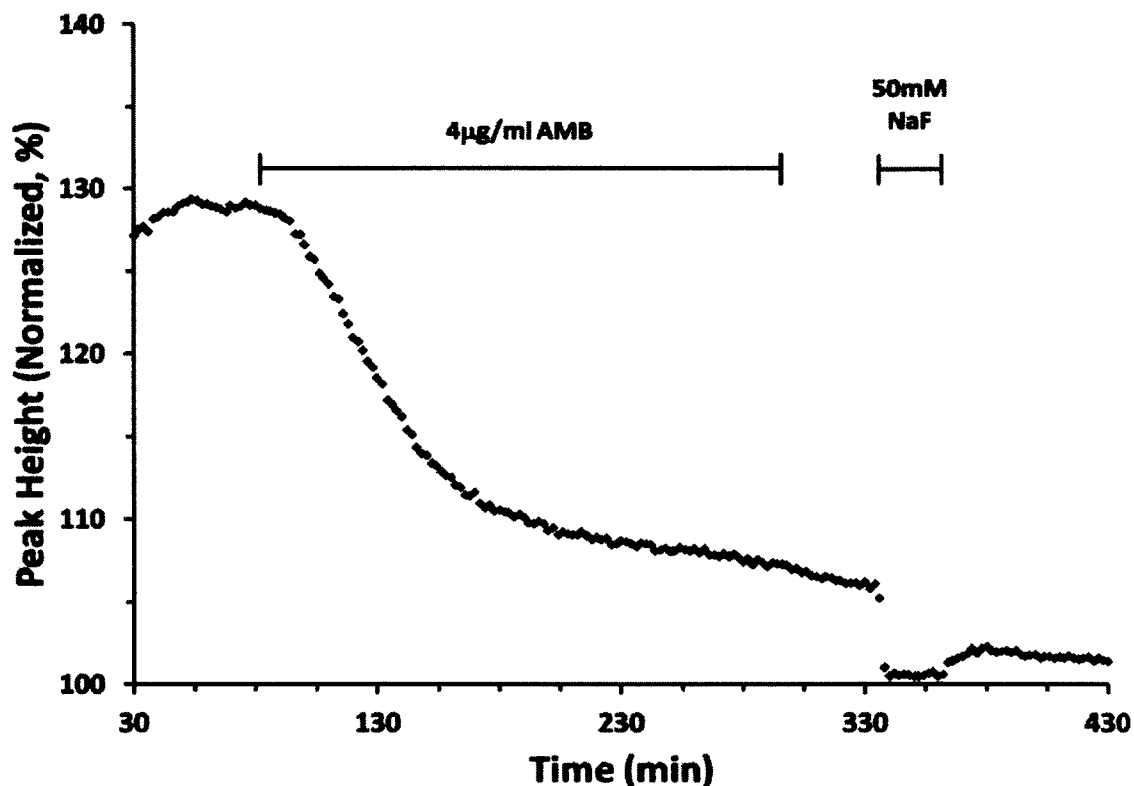


Figure 4.3. *C. albicans* response to 4 $\mu\text{g/ml}$ AMB (50 to 282 min) and 50mM NaF (338 to 360 min) using 90/30 s flow/stop cycle and 50% flow rate.

The effect of AMB can be observed as a decrease in the peak height after introduction at 50 min. This decrease was still observed after the AMB perfusion was discontinued at 282 min. This continued decrease could be because the leakage of ions from the cells might be still in progress and can be seen as a residual effect of AMB on *C. albicans* [84].

Next, 50 mM NaF was perfused from 338 to 360 min to observe how *C. albicans* under distress respond. As expected, a decrease in peak height was observed (Figure 4.3) when *C. albicans* came in contact with NaF. When the NaF perfusion was discontinued, the peak height did not return to its previous level, as seen in Figure 4.1. The change in peak level may be caused by the synergistic effect of AMB and NaF on the metabolism of *C. albicans*.

4.3.4 *C. albicans* Response to Miconazole

Next the measurement technique was used to observe the effect of an azole-based antifungal miconazole (MCZ). Azole-based antifungals are fungistatic because they repress the growth of *C. albicans*. Cells were plated in a 24-well plate and placed on the Cytosensor[®] platform. After acclimatization, 8 µg/ml of MCZ was perfused from 90 to 224 min and 50 mM NaF was perfused from 280 to 302 min. As seen in Figure 4.4, MCZ has little to no effect on the oxygen consumption rate of *C. albicans*. Interestingly, 50 mM NaF had no effect on the oxygen consumption rate, although our previous experiments (Figures 4.1, 4.2, and 4.3) had shown that 50 mM NaF was sufficient to cause a decrease in extracellular oxygen consumption.

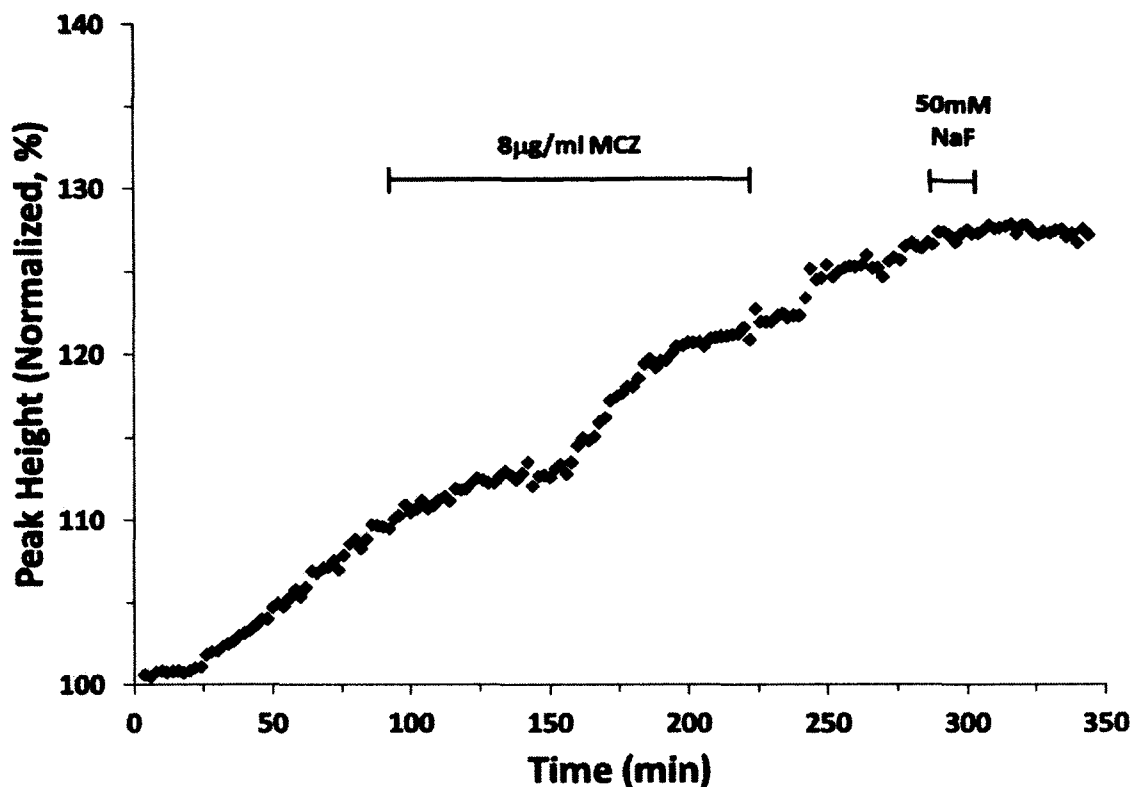


Figure 4.4. *C. albicans* response to 8 $\mu\text{g/ml}$ MCZ from 90 to 224 min and 50 mM NaF from 280 to 302 min using 90/30 s flow/stop cycle and 50% flow rate.

The lack of change with MCZ could be explained by results from Rogers et al. [85] who used an antifungal resistant and susceptible strain of *C. glabrata*, and measured the protein expression when exposed to fluconazole (FCZ) another azole. They reported a higher protein expression in the resistant strain. One of the up-regulated proteins was enolase, which is required during the glycolysis cycle and which also helps *C. albicans* to survive in the GI tract of humans [78][86].

4.3.5 *C. albicans* Response to Fluconazole

FCZ was used to determine if the same effect with NaF can be observed. The cells were allowed to reach a steady state, and 8 $\mu\text{g/ml}$ of FCZ was perfused from 72 to 314 min, followed by 50 mM NaF from 334 to 356 min as seen in Figure 4.5.

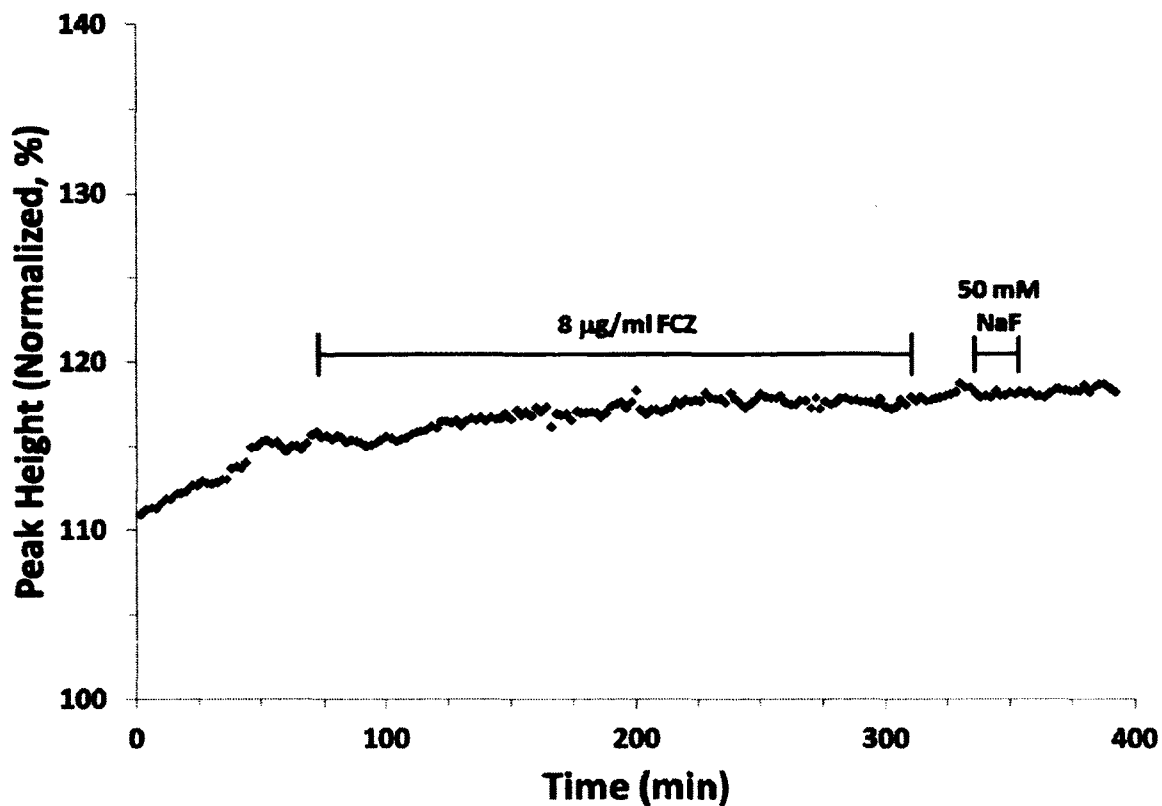


Figure 4.5. *C. albicans* response to 8 $\mu\text{g/ml}$ FCZ (72 to 314 min) and 50 mM NaF (334 to 356 min) using 90/30 s flow/stop cycle and 50% flow rate.

As seen in Figure 4.5, after the introduction of FCZ, extracellular oxygen consumption by *C. albicans* did not change. The cell metabolism reached a steady state at ~ 180 min. No change was observed even after the introduction of 50 mM NaF. Similar response from *C. albicans* was observed in Figure 4.4 in the presence of another antifungal, MCZ. Next higher concentrations of NaF (200 mM) and FCZ (16 $\mu\text{g/ml}$) were used to observe if *C. albicans* had become completely resistant to NaF or if they remained susceptible. 16 $\mu\text{g/ml}$ FCZ was perfused from 96 to 342 min. As seen in Figure 4.6, although FCZ caused a slight decrease in the oxygen consumption, it eventually reached a steady state.

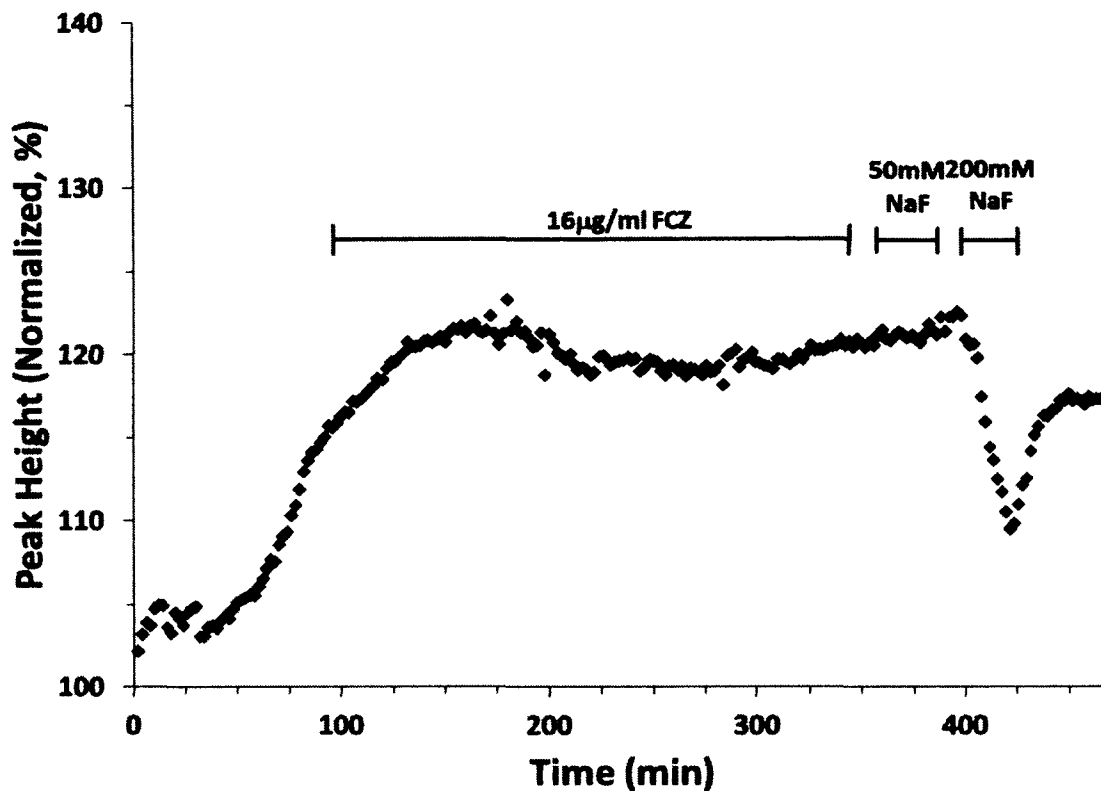


Figure 4.6. *C. albicans* response to 16 $\mu\text{g/ml}$ FCZ from 96 to 342 min, 50 mM NaF from 358 to 380 min, and 200 mM NaF from 398 to 420 min using 90/30 s flow/stop cycle and 50% flow rate.

Similar to the 8 $\mu\text{g/ml}$ MCZ, FCZ experiments, 50 mM NaF did not show an effect on the cell metabolism when perfused from 358 to 380 min. Interestingly, when 200 mM NaF was perfused from 398 to 420 min the oxygen consumption decreased. One explanation could be that the higher concentration of NaF is enough to counteract the upregulation of enolase enzyme by *C. albicans* to build up resistance to antifungals.

4.4 Conclusions

A novel method and measurement apparatus has been presented for detecting response of *C. albicans* in real-time when exposed to different antifungals such as AMB, MCZ and FCZ. This process does not require specialized cellular scaffolding as the

experiments can be performed in a 24-well plate familiar to researchers. As the measurement process is non-invasive, cells can be potentially used for other experiments after the fluorescence data are obtained. It has been shown that *C. albicans* oxygen consumption in general can be inhibited by NaF, an enolase inhibitor. But *C. albicans* treated with different antifungals (polyene and azole based) show different responses, where NaF has an effect on polyene treated antifungal like AMB, and it does not show an effect when treated with to azole based antifungals like MCZ and FCZ. Further work should be carried out to learn how *C. albicans* develops resistance to antifungals and also how they respond to NaF when treated with other families of antifungals at different concentrations.

5.0 FUTURE WORK

To make this sensor platform more useful, work should be carried out to develop other fluorescent thin film which can measure change in analytes like pH, glucose, calcium. Currently work is in progress to develop fluorescent films to incorporate into the measurement platform that can detect changes in pH and K^+ in addition to oxygen.

The sensor head design should also be modified to fit in 12, 48, 96-well plates. As a proof of concept we developed a 3D printed sensor head that fits in a 24-well plate. Free 3D design software Tinkercad (an online freeware) was used for this purpose, and the images are shown in Figure 5.1.

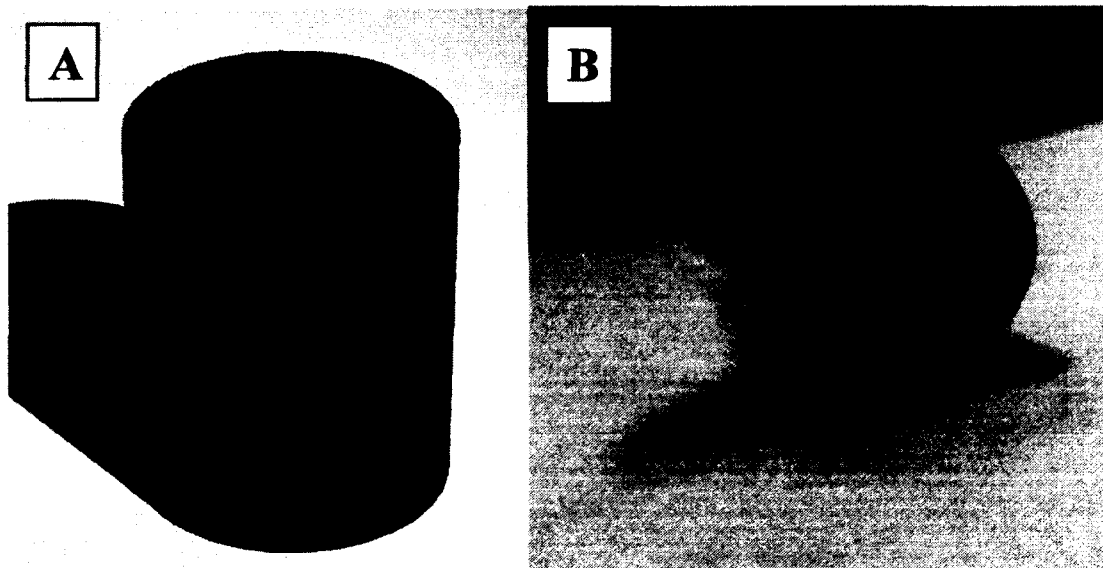


Figure 5.1. (A) Image of the sensor head 3D design from Tinkercad software, (B) 3D printed sensor head with fiber optic bundle and solution perfusion tubes.

An optical fiber bundle comprising one excitation fiber surrounded by six emission collection fibers was sealed in the 3D printed sensor head along with solution inlet and outlet perfusion tubes. The 3D printed sensor head was then used to observe oxygen consumption from *C. albicans* by using the same experiment conditions as used in the antifungal studies in Chapter 4. The raw data obtained using the 3D printed sensor head is shown in Figure 5.2, where the fluorescent intensity signal during the stop flow cycle showing oxygen consumption of the cells is quite visible and comparable to the signal from the modified Cytosensor[®] head. However, the peak and baseline during flow appears to be noisier than previous studies using the modified Cytosensor[®] head. This increased noise may be due to the roughness of the printed sensor head surface (Figure 5.1, B) caused by the printing resolution of the 3D printer used.

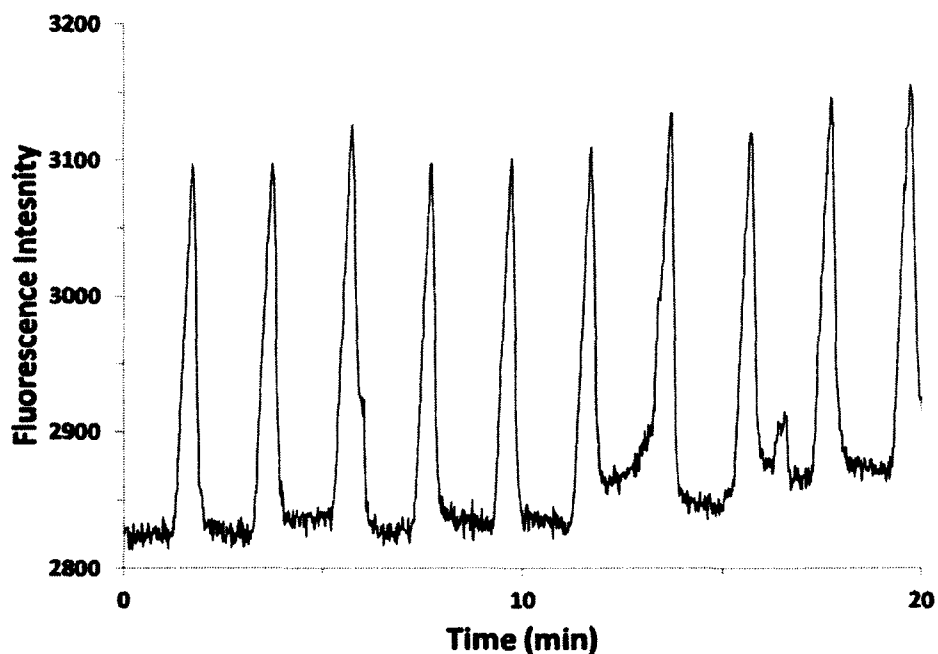


Figure 5.2. PtOEP film fluorescence response to *C. albicans* oxygen consumption during YPD media perfusion using a 90/30 s flow/stop cycle using the 3D printed sensor head.

After equilibration of the baseline metabolic rate was observed, the cells were exposed to 200 mM NaF (174 to 196 minutes) as seen in Figure 5.3, where a decrease in peak height can be observed. This decrease was in agreement with our hypothesis that the fluorescence intensity should decrease upon cell exposure to NaF in the perfusion media. When NaF perfusion was discontinued, the fluorescent intensity peaks during the stop cycles increased back to previous levels, indicating a recovery of cell metabolic activity as observed in Chapters 3 and 4.

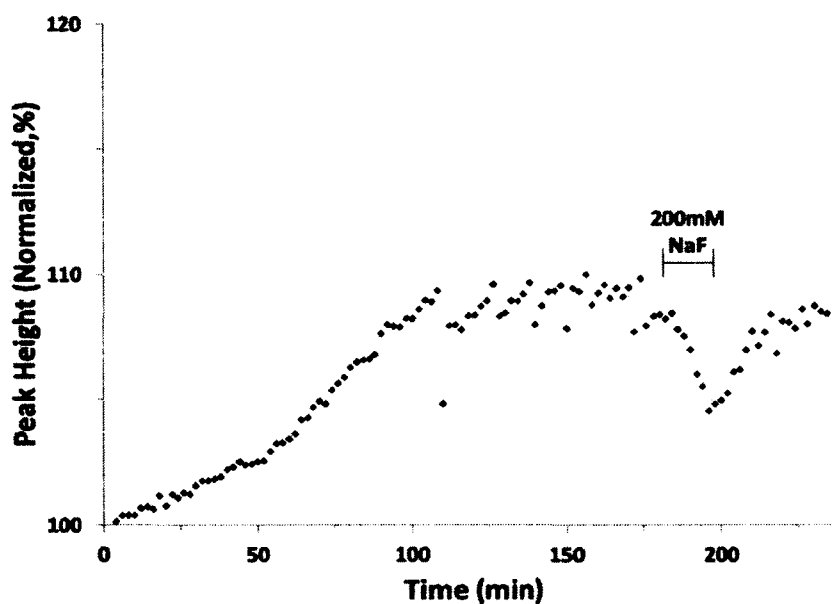


Figure 5.3. Effect of 200 mM NaF on the oxygen consumption of *C. albicans* during YPD media perfusion using a 90/30 s flow/stop cycle using the 3D printed sensor head.

Since the data from the 3D printed sensor head provided useful data in cell culture, we believe this will allow new sensor head designs to be rapidly prototyped, although the surface may need to be machined to create a smoother flow environment before the finalized design is die cast.

6.0 REFERENCES

- [1] H. McConnell, J. Owicki, J. Parce, D. Miller, G. Baxter, H. Wada, et al., The cytosensor microphysiometer: biological applications of silicon technology, *Science* (80-.). 257 (1992) 1906–1912.
- [2] S.E. Eklund, D. Taylor, E. Kozlov, A. Prokop, D.E. Cliffel, A microphysiometer for simultaneous measurement of changes in extracellular glucose, lactate, oxygen, and acidification rate., *Anal. Chem.* 76 (2004) 519–27.
- [3] D.A. Ferrick, A. Neilson, C. Beeson, Advances in measuring cellular bioenergetics using extracellular flux., *Drug Discov. Today.* 13 (2008) 268–74.
- [4] S.E. Eklund, R.M. Snider, J. Wikswo, F. Baudenbacher, A. Prokop, D.E. Cliffel, Multianalyte microphysiometry as a tool in metabolomics and systems biology, *J. Electroanal. Chem.* 587 (2006) 333–339.
- [5] S.J. Updike, G.P. Hicks, The Enzyme Electrode, *Nature.* 214 (1967) 986–988.
- [6] G.S.W. Anthony P. F. Turner, Isao Karube, *Biosensors: fundamentals and applications*, Oxford University Press, 1987.
- [7] L.M. Kauri, S.-K. Jung, R.T. Kennedy, Direct measurement of glucose gradients and mass transport within islets of Langerhans, *Biochem. Biophys. Res. Commun.* 304 (2003) 371–377.
- [8] S.-K. Jung, Correlated Oscillations in Glucose Consumption, Oxygen Consumption, and Intracellular Free Ca²⁺ in Single Islets of Langerhans, *J. Biol. Chem.* 275 (2000) 6642–6650.
- [9] F. Crespi, C. Möbius, In vivo selective monitoring of basal levels of cerebral dopamine using voltammetry with Nafion modified (NA-CRO) carbon fibre micro-electrodes., *J. Neurosci. Methods.* 42 (1992) 149–161.
- [10] B.P.H. Schaffar, Thick film biosensors for metabolites in undiluted whole blood and plasma samples., *Anal. Bioanal. Chem.* 372 (2002) 254–260.
- [11] J.W. Parce, J.C. Owicki, K.M. Kercso, G.B. Sigal, H.G. Wada, V.C. Muir, et al., Detection of cell-affecting agents with a silicon biosensor., *Science.* 246 (1989) 243–247.

- [12] J.C. Owicki, J.W. Parce, K.M. Kercso, G.B. Sigal, V.C. Muir, J.C. Venter, et al., Continuous monitoring of receptor-mediated changes in the metabolic rates of living cells., *Proc. Natl. Acad. Sci. U. S. A.* 87 (1990) 4007–4011.
- [13] I. Karube, T. Matsunaga, S. Suzuki, Microbioassay of nystatin with a yeast electrode, *Anal. Chim. Acta.* 109 (1979) 39–44.
- [14] Susan R Mikkelsen, *Bioelectrochemistry*, Vol 9, Wiley-VCH: Weinheim, 2002.
- [15] J.C. Owicki, J. Wallace Parce, Biosensors based on the energy metabolism of living cells: The physical chemistry and cell biology of extracellular acidification, *Biosens. Bioelectron.* 7 (1992) 255–272.
- [16] F. Hafner, Cytosensor Microphysiometer: technology and recent applications., *Biosens. Bioelectron.* 15 (2000) 149–58.
- [17] S. Pitchford, Ligand characterization using microphysiometry., *Curr. Protoc. Neurosci.* Chapter 7 (2001) Unit7.8.
- [18] J.M. Arthur, G.P. Collinsworth, T.W. Gettys, L.D. Quarles, J.R. Raymond, Specific coupling of a cation-sensing receptor to G protein alpha-subunits in MDCK cells, *Am J Physiol Ren. Physiol.* 273 (1997) F129–135.
- [19] K. Burvall, L. Palmberg, K. Larsson, Metabolic activation of A549 human airway epithelial cells by organic dust: A study based on microphysiometry, *Life Sci.* 71 (2002) 299–309.
- [20] D. Smart, M.D. Wood, Cytosensor techniques for examining signal transduction of neurohormones, *Biochem. Cell Biol.* (2011).
- [21] B. Stein, M. George, H. Gaub, J. Behrends, W. Parak, Spatially resolved monitoring of cellular metabolic activity with a semiconductor-based biosensor, *Biosens. Bioelectron.* 18 (2003) 31–41.
- [22] S.E. Eklund, R.G. Thompson, R.M. Snider, C.K. Carney, D.W. Wright, J. Wikswo, et al., Metabolic discrimination of select list agents by monitoring cellular responses in a multianalyte microphysiometer., *Sensors (Basel).* 9 (2009) 2117–2133.
- [23] E.A. Lima, R.M. Snider, R.S. Reiserer, J.R. McKenzie, D.W. Kimmel, S.E. Eklund, et al., Multichamber Multipotentiostat System for Cellular Microphysiometry., *Sens. Actuators. B. Chem.* 204 (2014) 536–543.
- [24] N.M.M. Pires, T. Dong, U. Hanke, N. Hoivik, Recent developments in optical detection technologies in lab-on-a-chip devices for biosensing applications., *Sensors (Basel).* 14 (2014) 15458–15479.

- [25] J.R. Lakowicz, ed., *Principles of Fluorescence Spectroscopy*, Springer US, Boston, MA, 2006.
- [26] R.J. Reiffenstein, W.C. Hulbert, S.H. Roth, Toxicology of hydrogen sulfide., *Annu. Rev. Pharmacol. Toxicol.* 32 (1992) 109–134.
- [27] J.C. Pickup, F. Hussain, N.D. Evans, O.J. Rolinski, D.J.S. Birch, Fluorescence-based glucose sensors, 20 (2005) 2555–2565.
- [28] K. Waich, T. Mayr, I. Klimant, Fluorescence sensors for trace monitoring of dissolved ammonia., *Talanta.* 77 (2008) 66–72.
- [29] S.M. Grist, L. Chrostowski, K.C. Cheung, Optical oxygen sensors for applications in microfluidic cell culture., *Sensors (Basel).* 10 (2010) 9286–9316.
- [30] H. Xu, J.W. Aylott, R. Kopelman, T.J. Miller, M.A. Philbert, A Real-Time Ratiometric Method for the Determination of Molecular Oxygen Inside Living Cells Using Sol–Gel-Based Spherical Optical Nanosensors with Applications to Rat C6 Glioma, *Anal. Chem.* 73 (2001) 4124–4133.
- [31] S.M. Buck, H. Xu, M. Brasuel, M. a Philbert, R. Kopelman, Nanoscale probes encapsulated by biologically localized embedding (PEBBLEs) for ion sensing and imaging in live cells., *Talanta.* 63 (2004) 41–59.
- [32] K. Hanson, Rethinking the Jablonski Diagram, <http://www.chemistry-blog.com/2013/11/09/rethinking-the-jablonski-diagram/> (accessed May 19, 2015).
- [33] J. Snider, Fluorescent Probes, <https://www.lifetechnologies.com/us/en/home/life-science/protein-biology/protein-biology-learning-center/protein-biology-resource-library/pierce-protein-methods/fluorescent-probes.html#/legacy=www.piercenet.com> (accessed May 29, 2015).
- [34] A.R. Barron, L. Li, OpenStax CNX - The Application of Fluorescence Spectroscopy in the Mercury Ion Detection, http://cnx.org/contents/422b0076-5576-48ee-a400-8445b1b8102c@1/The_Application_of_Fluorescenc (accessed May 2, 2015).
- [35] O. Optics, USB4000 Fiber Optic Spectrometer Installation and Operation Manual, Doc. Number 211-00000-000-02-0908. (2008) 27–30.
- [36] R. Ramamoorthy, P.K. Dutta, S.A. Akbar, Oxygen sensors: Materials, methods, designs and applications, *J. Mater. Sci.* 38 (n.d.) 4271–4282.
- [37] L.C. Clark, W. R, D. Granger, Z. Taylor, Continuous recording of blood oxygen tensions by polarography., *J. Appl. Physiol.* 6 (1953) 189–193.

- [38] A. Mills, A. Lepre, Controlling the Response Characteristics of Luminescent Porphyrin Plastic Film Sensors for Oxygen, *Anal. Chem.* 69 (1997) 4653–4659.
- [39] C.-S. Chu, Y.-L. Lo, T.-W. Sung, Review on recent developments of fluorescent oxygen and carbon dioxide optical fiber sensors, *Photonic Sensors.* 1 (2011) 234–250.
- [40] S. Lee, I. Okura, Photostable Optical Oxygen Sensing Material : Platinum Tetrakis (pentafluorophenyl) porphyrin Immobilized in Polystyrene, 34 (1997) 185–188.
- [41] M. Quaranta, S.M. Borisov, I. Klimant, Indicators for optical oxygen sensors., *Bioanal. Rev.* 4 (2012) 115–157.
- [42] R. Ciriminna, M. Pagliaro, Organofluoro-silica xerogels as high-performance optical oxygen sensors., *Analyst.* 134 (2009) 1531–1535.
- [43] Y. Amao, T. Miyashita, I. Okura, Optical oxygen sensing based on the luminescence change of metalloporphyrins immobilized in styrene–pentafluorostyrene copolymer film, *Analyst.* 125 (2000) 871–875.
- [44] D.A. Chang-Yen, A. Badardeen, B.K. Gale, Spin-assembled nanofilms for gaseous oxygen sensing, *Sensors Actuators B Chem.* 120 (2007) 426–433.
- [45] P. Hartmann, W. Ziegler, G. Holst, D.W. Lübbers, Oxygen flux fluorescence lifetime imaging, *Sensors Actuators B Chem.* 38 (1997) 110–115.
- [46] G. Liebsch, I. Klimant, B. Frank, G. Holst, O.S. Wolfbeis, Luminescence Lifetime Imaging of Oxygen, pH, and Carbon Dioxide Distribution Using Optical Sensors, *Appl. Spectrosc.* 54 (2000) 548–559.
- [47] D.B. Papkovsky, R.I. Dmitriev, Biological detection by optical oxygen sensing., *Chem. Soc. Rev.* 42 (2013) 8700–8732.
- [48] C. O'Donovan, J. Hynes, D. Yashunski, D.B. Papkovsky, Phosphorescent oxygen-sensitive materials for biological applications, *J. Mater. Chem.* 15 (2005) 2946.
- [49] E.J. Park, M. Brasuel, C. Behrend, M. a Philbert, R. Kopelman, Ratiometric optical PEBBLE nanosensors for real-time magnesium ion concentrations inside viable cells., *Anal. Chem.* 75 (2003) 3784–3791.
- [50] Y.-E.L. Koo, Y. Cao, R. Kopelman, S.M. Koo, M. Brasuel, M.A. Philbert, Real-time measurements of dissolved oxygen inside live cells by organically modified silicate fluorescent nanosensors., *Anal. Chem.* 76 (2004) 2498–2505.

- [51] K. Kellner, G. Liebsch, I. Klimant, O.S. Wolfbeis, T. Blunk, M.B. Schulz, et al., Determination of oxygen gradients in engineered tissue using a fluorescent sensor., *Biotechnol. Bioeng.* 80 (2002) 73–83.
- [52] G. Holst, B. Grunwald, Luminescence lifetime imaging with transparent oxygen optodes, *Sensors Actuators B Chem.* 74 (2001) 78–90.
- [53] S. Gatti, T. Brey, W.E.G. Müller, O. Heilmayer, G. Holst, Oxygen microoptodes: a new tool for oxygen measurements in aquatic animal ecology, *Mar. Biol.* (2002).
- [54] E.J. Park, K.R. Reid, W. Tang, R.T. Kennedy, R. Kopelman, Ratiometric fiber optic sensors for the detection of inter- and intra-cellular dissolved oxygen, *J. Mater. Chem.* 15 (2005) 2913.
- [55] F. Chen, Q. Xia, L.-K. Ju, Competition between oxygen and nitrate respirations in continuous culture of *Pseudomonas aeruginosa* performing aerobic denitrification., *Biotechnol. Bioeng.* 93 (2006) 1069–1078.
- [56] T. Klein, K. Schneider, E. Heinzle, A system of miniaturized stirred bioreactors for parallel continuous cultivation of yeast with online measurement of dissolved oxygen and off-gas., *Biotechnol. Bioeng.* 110 (2013) 535–542.
- [57] T.-S. Yeh, C.-S. Chu, Y.-L. Lo, Highly sensitive optical fiber oxygen sensor using Pt(II) complex embedded in sol–gel matrices, *Sensors Actuators B Chem.* 119 (2006) 701–707.
- [58] J.R. Lakowicz, *Principles of Fluorescence Spectroscopy*, 3rd Edition, Springer. (2006).
- [59] I. Klimant, M. Köhl, R.N. Glud, G. Holst, Optical measurement of oxygen and temperature in microscale: strategies and biological applications, *Sensors Actuators B Chem.* 38 (1997) 29–37.
- [60] D.B. Papkovsky, J. Olah, I. V. Troyanovsky, N.A. Sadovsky, V.D. Rummyantseva, A.F. Mironov, et al., Phosphorescent polymer films for optical oxygen sensors, *Biosens. Bioelectron.* 7 (1992) 199–206.
- [61] C.W.P. Donald Voet, Judith G. Voet, *Fundamentals of Biochemistry*, John Wiley and Sons, New York, 1999.
- [62] S. Flisfisch, J. Meyer, J.H. Meurman, T. Waltimo, Effects of fluorides on *Candida albicans*., *Oral Dis.* 14 (2008) 296–301.
- [63] O. Barbier, L. Arreola-Mendoza, L.M. Del Razo, Molecular mechanisms of fluoride toxicity., *Chem. Biol. Interact.* 188 (2010) 319–33.

- [64] P.A.B. Orlean, S.M. Ward, Sodium fluoride stimulates (1,3)- β -D-glucan synthase from, 18 (1983) 31–35.
- [65] J.K. Hongslo, R.I. Holland, J. Jonsen, Effect of Sodium Fluoride on LS Cells, *J. Dent. Res.* 53 (1974) 410–413.
- [66] A. Rodaki, I.M. Bohovych, B. Enjalbert, T. Young, F.C. Odds, N.A.R. Gow, et al., Glucose promotes stress resistance in the fungal pathogen *Candida albicans*., *Mol. Biol. Cell.* 20 (2009) 4845–4855.
- [67] J. Berman, P.E. Sudbery, *Candida albicans*: a molecular revolution built on lessons from budding yeast., *Nat. Rev. Genet.* 3 (2002) 918–930.
- [68] I.K. Maurya, C.K. Thota, S.D. Verma, J. Sharma, M.K. Rawal, B. Ravikumar, et al., Rationally designed transmembrane peptide mimics of the multidrug transporter protein Cdr1 act as antagonists to selectively block drug efflux and chemosensitize azole-resistant clinical isolates of *Candida albicans*., *J. Biol. Chem.* 288 (2013) 16775–16787.
- [69] C.-C. Lai, C.-K. Tan, Y.-T. Huang, P.-L. Shao, P.-R. Hsueh, Current challenges in the management of invasive fungal infections., *J. Infect. Chemother.* 14 (2008) 77–85.
- [70] S.M. Noble, A.D. Johnson, Genetics of *Candida albicans*, a diploid human fungal pathogen., *Annu. Rev. Genet.* 41 (2007) 193–211.
- [71] D. Sanglard, F. Ischer, T. Parkinson, D. Falconer, J. Bille, *Candida albicans* mutations in the ergosterol biosynthetic pathway and resistance to several antifungal agents., *Antimicrob. Agents Chemother.* 47 (2003) 2404–2412.
- [72] A.M. Sugar, Use of amphotericin B with azole antifungal drugs: what are we doing?, *Antimicrob. Agents Chemother.* 39 (1995) 1907–1912.
- [73] B.E. Mansfield, H.N. Oltean, B.G. Oliver, S.J. Hoot, S.E. Leyde, L. Hedstrom, et al., Azole drugs are imported by facilitated diffusion in *Candida albicans* and other pathogenic fungi., *PLoS Pathog.* 6 (2010) e1001126.
- [74] K.C. Gray, D.S. Palacios, I. Dailey, M.M. Endo, B.E. Uno, B.C. Wilcock, et al., Amphotericin primarily kills yeast by simply binding ergosterol., *Proc. Natl. Acad. Sci. U. S. A.* 109 (2012) 2234–2239.
- [75] R.E. Lewis, Current concepts in antifungal pharmacology., *Mayo Clin. Proc.* 86 (2011) 805–817.

- [76] T.T. Liu, R.E.B. Lee, K.S. Barker, R.E. Lee, L. Wei, R. Homayouni, et al., Genome-wide expression profiling of the response to azole, polyene, echinocandin, and pyrimidine antifungal agents in *Candida albicans*., *Antimicrob. Agents Chemother.* 49 (2005) 2226–2236.
- [77] A. Voss, R.J. Hollis, M.A. Pfaller, R.P. Wenzel, B.N. Doebbeling, Investigation of the sequence of colonization and candidemia in nonneutropenic patients., *J. Clin. Microbiol.* 32 (1994) 975–980.
- [78] R.C. Silva, A.C.B. Padovan, D.C. Pimenta, R.C. Ferreira, C. V da Silva, M.R.S. Briones, Extracellular enolase of *Candida albicans* is involved in colonization of mammalian intestinal epithelium., *Front. Cell. Infect. Microbiol.* 4 (2014) 66.
- [79] F.C. Donofrio, A.C.A. Calil, E.T. Miranda, A.M.F. Almeida, G. Benard, C.P. Soares, et al., Enolase from *Paracoccidioides brasiliensis*: isolation and identification as a fibronectin-binding protein., *J. Med. Microbiol.* 58 (2009) 706–713.
- [80] M. Nucci, E. Anaissie, Revisiting the source of candidemia: skin or gut?, *Clin. Infect. Dis.* 33 (2001) 1959–1967.
- [81] L. Angiolella, M. Facchin, A. Stringaro, B. Maras, N. Simonetti, A. Cassone, Identification of a glucan-associated enolase as a main cell wall protein of *Candida albicans* and an indirect target of lipopeptide antimycotics., *J. Infect. Dis.* 173 (1996) 684–690.
- [82] P. Sundstrom, J. Jensen, E. Balish, Humoral and Cellular Immune Responses to Enolase after Alimentary Tract Colonization or Intravenous Immunization with *Candida albicans*, *J. Infect. Dis.* 170 (1994) 390–395.
- [83] J.H. Jeng, C.C. Hsieh, W.H. Lan, M.C. Chang, S.K. Lin, L.J. Hahn, et al., Cytotoxicity of sodium fluoride on human oral mucosal fibroblasts and its mechanisms, *Cell Biol. Toxicol.* 14 (1998) 383–389.
- [84] V. Moudgal, J. Sobel, Antifungals to treat *Candida albicans*., *Expert Opin. Pharmacother.* 11 (2010) 2037–2048.
- [85] P.D. Rogers, J.-P. Vermitsky, T.D. Edlind, G.M. Hilliard, Proteomic analysis of experimentally induced azole resistance in *Candida glabrata*., *J. Antimicrob. Chemother.* 58 (2006) 434–438.
- [86] D.P. Kontoyiannis, R.E. Lewis, Antifungal drug resistance of pathogenic fungi, *Lancet.* 359 (2002) 1135–1144.